ANALYSIS OF PLATOON IMPACTS ON LEFT-TURN DELAY

AT UNSIGNALIZED INTERSECTIONS

A Thesis

by

FENG WAN

Submitted to the Office of Graduate Studies of
Texas A&M University
in partial fulfillment of the requirements for the degree of

MASTER OF SCIENCE

December 2010

Major Subject: Civil Engineering

Analysis of Platoon Impacts on Left-Turn Delay at Unsignalized Intersections

ANALYSIS OF PLATOON IMPACTS ON LEFT-TURN DELAY

AT UNSIGNALIZED INTERSECTIONS

A Thesis

by

FENG WAN

Submitted to the Office of Graduate Studies of
Texas A&M University
in partial fulfillment of the requirements for the degree of

MASTER OF SCIENCE

Approved by:

Chair of Committee,   Yunlong Zhang
Committee Members,   Dominique Lord
                            Clifford Spiegelman
Head of Department,   John Niedzwecki

December 2010

Major Subject: Civil Engineering

ABSTRACT

Analysis of Platoon Impacts on Left-Turn Delay

at Unsignalized Intersections. (December 2010)

Feng Wan, B.S., Tongji University

Chair of Advisory Committee: Dr. Yunlong Zhang

Traffic platoons created by traffic signals may have impacts on the operations of downstream intersections because they change the arrival pattern and gap distribution of upstream traffic. There's been a lot of research dealing with platoon effects on operations at signalized intersections, while very limited research has been done for that of unsignalized intersections.

This research aims to develop a methodology for analyzing the platoon impacts on major-street left-turn (MSLT) delay at two-way stop-controlled (TWSC) intersections. The main idea is using a microscopic simulation tool to simulate different platoon scenarios in opposing through traffic, then applying regression models to capture the impacts of platoons on the delay of MSLT. Two platoon variables were adopted as a simplification of the complex platoon scenarios, making it practical to analyze the platoon effects on MSLT delay.

The first two steps were to build simulation models for real-world unsignalized intersections and simulate scenarios with a combination of various factors related to platoons in VISSIM simulation. Calibrations of these simulation models based on field

data were performed before simulation started. The next step was to define, derive and calibrate two platoon variables for describing the duration and intensity of platoon arrivals in the opposing through traffic, which effectively simplified the large combination of various factors. At last, the two platoon variables and their relationship with MSLT delay change factor were modeled with regression tools. A relationship between the two variables and the delay change factor was established, which indicated a positive effect by upstream platoons on MSLT delay and made it possible to quantify the impacts. The findings in this research could also be used for future research on left-turn treatment regarding platoon or signal impacts.

DEDICATION

This is dedicated to all transportation engineers! We accelerate the world!

ACKNOWLEDGEMENTS

Association of State Highway and Transportation Officials, or the individual states

participating in the National Cooperative Highway Research Program.

NOMENCLATURE

AWSC   All-Way Stop-Controlled

LOS   Level-of-Service

LTL   Left-Turn Lane

MOE   Measure-of-Effectives

MSLT   Major-Street Left-Turn

TWSC   Two-Way Stop-Controlled

vphpl   Vehicles per Hour per Lane

TABLE OF CONTENTS

LIST OF FIGURES

LIST OF TABLES

CHAPTER I

INTRODUCTION

Background

The left-turn movement at an intersection has always been a major issue for both traffic operation and safety of an intersection. At intersections with traffic volumes high enough to satisfy traffic signal warrants, traffic signals are often installed and left turn movements may be protected depending on the left-turn and opposing through volumes. At unsignalized intersections, left-turns are made safely only when sufficiently large gaps are present in opposing through traffic. Because of this, left-turn delay is common and left-turn operations are more restricted than other movements at unsignalized intersections.

In this research, the interest centers on the major-street left-turn (MSLT) movement at a two-way stop-controlled (TWSC) intersection. The analysis of delay and other operational or safety variables are essential for the level-of-service (LOS) and safety performance at an unsignalized intersection. Left-turn delay is dependent upon left-turn and opposing through movement volumes, gap distributions, critical gaps, and intersection geometry. In addition to the demand levels of left-turn and opposing through movements, the arrival patterns of opposing through vehicles could also be a significant factor affecting left-turn delay because it changes the gap distribution.

_____

This thesis follows the style of *Transportation Research Record*.

A traffic signal discharges vehicles primarily on green times, with vehicles often leaving the intersection on green in platoons. Platoons might have a significant impact on the gap distribution of through vehicles and further affect the MSLT movement delay at the downstream intersection. The effects of platoons generated from the upstream signal intersection on MSLT delay are investigated in this research. VISSIM simulation is selected as the platform for research and field data is used to calibrate VISSIM simulation.

In order to get reliable simulation results from VISSIM, the parameters should be carefully calibrated before performing the simulation. Delay calculations for left-turn movements at unsignalized intersections are based on gap acceptance theory in the 2000 Highway Capacity Manual [1], and critical gap and follow-up time are the two fundamental parameters of the gap acceptance model. The calibration in this research was based on the extensive database established for the NCHRP 3-91 project, Left-Turn Accommodations at Unsignalized Intersections. 30 TWSC unsignalized intersections in three states of United States (Texas, Arizona, and New York) were videotaped with DV cameras, out of which useful data was extracted. Raff's critical gap model and logistic regression model were employed to calibrate and analyze the critical gaps in this research.

Statement of Problem

As mentioned above, the platoons may have impacts on left-turn operations at the downstream unsignalized intersection. Particularly, the platoon effects on the delay to

the major-street left-turn movement at the downstream TWSC intersection will be investigated in this research. While unsignalized intersections include both two-way stop-controlled (TWSC) and all-way stop-controlled (AWSC) intersections, this research focuses on just the TWSC intersections. Very limited research has been done on this topic, and therefore further research is demanded.

Purpose of the Study

The objective of this research is to develop a methodology for estimating the platoon effects on the MSLT operations at TWSC intersections and provide recommendations for left-turn treatment at unsignalized intersections. Goals to achieve include:

- calibrating and updating critical gap values for the left-turn operation for unsignalized intersections,

- designing analysis on the platoon impacts on MSLT delays,

- developing the methodology for estimating the platoon effects, and

- making recommendations on left-turn treatments based on the simulation results.

Organization of the Thesis

The paper is organized as follows. Chapter I gives a brief introduction to the research that will be performed. Chapter II describes documented literatures that are related to the analysis of platoon effects on left-turn delay at unsignalized intersections.

Chapter III briefs the datasets prepared in this research. Chapter IV is the methodology part, which includes the description of the data collection, approach of simulation and method of analysis. Chapter V and Chapter VI present the results and the main conclusions of the research. Finally, limitations and future work are documented in Chapter VII.

CHAPTER II

LITERATURE REVIEW

Platoon Effect

Traffic signals discharge queues on green time and cause vehicles to travel in platoons at the signalized intersection. Platooning traffic has quite different characteristics in arrival pattern and gap distribution from random-arriving traffic. Therefore the operation of intersections might be affected by platoons, and the effect has been proven at signalized intersections. In HCM 2000, the concepts of arrival pattern and progression adjustment factor were introduced to account for the impacts of platoons on the delay at signalized intersections [1].

The platoon ratio (R_p) is estimated using the formula in Equation 1 [1].The approximate ranges of Platoon Ratio (R_p) are related to arrival type as shown in Table 1, and default values are suggested for use in subsequent computations in Table 2.

The progression adjustment factor (PF) applies to all coordinated lane groups, including both pre-timed control and non-actuated lane groups in semi-actuated control systems. Progression primarily affects uniform delay, and for this reason, the adjustment is applied only to d_1. The value of PF may be determined using Equation 2.

$$R_p = \frac{P}{g/C} \tag{1}$$

$$PF = \frac{(1-P)f_{PA}}{1-(\frac{g}{C})}$$
(2)

where

PF = progression adjustment factor,
P = proportion of vehicles arriving on green,
g/C = proportion of green time available, and
f_{pA} = supplemental adjustment factor for platoon arriving during green.

Alternatively, Table 2 may also be used to determine PF as a function of the arrival type based on the default values for P and f_{PA} associated with each arrival type. The value of P may be measured in the field or estimated from the arrival type.

Table 1 Relationship between Arrival Type and Platoon Ratio (R_p)

Arrival Type	Range of Platoon Ratio (R_p)	Default Value (R_p)	Progression Quality
1	< 0.50	0.333	Very poor
2	> 0.50–0.85	0.667	Unfavorable
3	> 0.85–1.15	1.000	Random arrivals
4	> 1.15-1.50	1.333	Favorable
5	> 1.50–2.00	1.667	Highly favorable
6	> 2.00	2.000	Exceptional

Table 2 Progression Adjustment Factor for Uniform Delay Calculation

Green Ratio (g/C)	AT 1	AT 2	AT 3	AT 4	AT 5	AT 6
0.2	1.167	1.007	1.000	1.000	0.833	0.750
0.3	1.286	1.063	1.000	0.986	0.714	0.571
0.4	1.445	1.136	1.000	0.895	0.555	0.333
0.5	1.667	1.240	1.000	0.767	0.333	0.000
0.6	2.001	1.395	1.000	0.576	0.000	0.000
0.7	2.556	1.653	1.000	0.256	0.000	0.000
f_{PA}	1.00	0.93	1.00	1.15	1.00	1.00
Default R_p	0.333	0.667	1.000	1.333	1.667	2.000

Note*:   1. $PF = (1-P) f_{PA} / (1- g/C)$
2. Tabulation is based on default values of f_{PA} and R_p
3. $P = Rp * g/C$ (may not exceed 1.0)
4. PF may not exceed 1.0 for AT 3 through AT 6.

Actually, platoons change the gap distribution of vehicles and affect the operations of non-priority movements at downstream unsignalized intersections as well. However, very limited research has been done on platoon effects on the traffic operations of unsignalized intersections. Positive effects of platoons on nonpriority capacity were found [2, 3]. Bonneson' method employed the platoon dispersion model to calculate the blocked time proportion and then estimate major-street left-turn capacity and delay at an unsignalized intersection with an upstream traffic signal [2]. This approach was later adopted in the 2000 version of the Highway Capacity Manual to model platoon effect on the minor traffic streams at unsignalized intersections [1]. However, this method was based on the assumption that no adequate gaps exist during blocked time; in reality, usable gaps may exist due to the platoon dispersion.

Tools that recognize platoons were developed to facilitate the research on platoons. Platoon identifiers were based on two user-specified threshold parameters:

maximum headway between two vehicles and the minimum number of vehicles that constitute a platoon. These limitations were typically used in platoon identification algorithms [*4, 5*]. An important characteristic of platoons is that they disperse when they travel. Models have been proposed to handle this dispersion, the TRANSYT-7F model being the most well known. The first platoon dispersion model was in a recursive form, which calculated the flow rate at a time interval based the previous interval [*6*]. Later, a closed-form platoon dispersion model was developed, which allowed direct application in analytical models [*7*].

Left-turn Operations

Modeling left-turn operations at unsignalized intersections has always been a challenge. The first well-known research on the operational analysis of left-turn movement was done by Harmelink. Left-turn warrants were published on the basis of queuing model with arrival and service rates assumed to be negative exponentially distributed [*8*]. Harmelink's warrants stated that the probability of a through vehicle arriving behind a stopped, left-turning vehicle should not exceed 0.02 for 40 mph, 0.015 for 50 mph, and 0.01 for 60. The final criteria were presented in the form of graphs with advancing volume, opposing volume, operating speed, and left-turn percentage. One example graph of Harmelink's criteria for determining the need for left-turn lanes is shown in Figure 1.
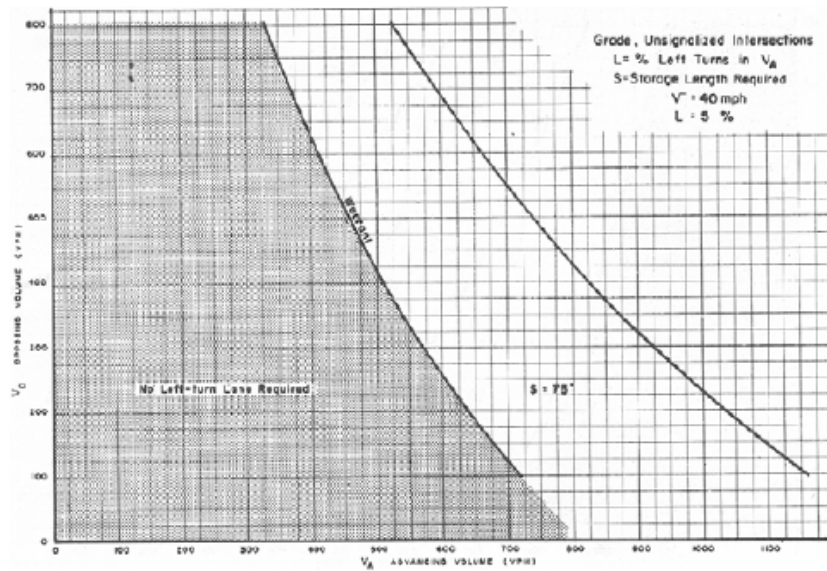
Figure 1 Harmelink – Left-Turn Warrant Graph 40 mph, 5% Left Turns, 1967

Most of the methods currently used to warrant left-turn lanes are based on Harmelink's model, but the values of traffic flow parameters suggested by Harmelink should be modified [*9*]. A decision support system for predicting benefits of left-turn lanes at unsignalized intersections was developed based on microscopic simulation and neural networks training [*10*].

One of the most important measures for left-turn operations is delay. The HCM 2000 defines control delay as the measure of effectives (MOEs) for the LOS of unsignalized intersections [*1*]. In this research, control delay was selected as the major MOE.

Also there's some research work on left-turn movement treatment from safety aspect conducted in the past. In general, left-turn lanes were found to be effective in reducing total crashes at intersections. A study showed that accident reductions from

18% to 77% by adding left-turn lanes [*11*]. At signalized intersection, left-turn lanes were observed to reduce accident rate by 6% with permitted phasing and by 35% with protected/permitted phasing [*12*]. The installation of left-turn lanes was also helping to reduce left-turn crashes [*13*]. The researchers also found that at intersections with left-turn lanes, rear-end, sideswipe, and left-turn crashes were reduced compared to intersections without left-turn lanes, but right-angle crashes increased [*14*].Another research team found that added left-turn lanes were effective in reducing total crashes as well as fatal and injury crashes [*15*].

Critical Gap Calibration

Critical gap was defined as the minimum time interval in the major-street traffic stream that allows intersection entry for one minor-street vehicle [*1*]. The HCM 2000 gave a set of critical gap and follow-up time values as shown in Table 3, calibrated based on the U.S. conditions. 4.1 sec was the critical gap recommended for MSLT movements at both two-lane and four-lane TWSC intersections. The problem with this critical gap is that it doesn't reflect the impacts of various factors.

Table 3 The 2000 HCM Critical Gaps and Follow-Up Times at TWSC Intersections

Vehicle Maneuver	Critical Gap t_c		Follow-Up Time t_f
	Two-Lane Major Road	Four Lane Major Road	
Left turn, major street	4.1	4.1	2.2
Right turn, minor street	6.2	6.9	3.3
Through, minor street	6.5	6.5	4.0
Left turn, minor street	7.1	7.5	3.5

For estimating the critical gaps, many different models have been proposed over the past sixty years. Brilon et al. [16] gave an overview of important critical gaps calibration models, among which the models of Siegloch (1973), Raff et al. (1950), Aworth (1970), Harders (1968), Hewett (1983), and Troutbeck (1992) were the most important ones. In practice, the most commonly used models were that of Raff et al. (1950) and Troutbeck (1992). In this research, Raff's model was employed to calibrate the critical gaps.

There are some methods summarized as logistic or logit models. The logit model was used a lot to study highway-design and safety issues. Lee and Mannering [17] employed a nested logit model to study the effect of roadside features on run-off-road accident severity. Chang and Mannering [18] used accident data to estimate a nested logit model of vehicle occupancy and accident severity. In the overview by Brilon et al. [16], the process of applying the logit model to calibrate the critical gap was introduced. Polus et al. [19] applied a disaggregate logit model to study the effect of waiting time at an approach to a roundabout on critical gaps. In this research, the logistic regression model was employed to identify the factors that affect critical gaps.

Critical gap has been found affected by some factors. For minor-street movement at unsignalized intersections, high delay was found to reduce the length of critical gap [20]. The same impact was found on roundabouts by Polus et al [19]. Driver ages were found to have some impact on the critical gaps, and the older drivers were found adopt significant longer critical gap values during nighttime [21]. The older drivers, especially older female drivers, displayed a conservative driving attitude as a compensation for

reduced driving ability [*22*]. In this research, factors examined included intersection geometry, posted speed limit, delay (waiting time) and some others.

Summary

Through the literature review, this research is positioned to develop a methodology which can accurately and easily identify the impacts of platooning traffic on the operations of MSLT movement at TWSC intersections. Delay is selected as the major measure of left-turn operations at unsignalized intersection in the presence of upstream signals. The analysis of platoon scenarios at unsignalized intersections will be the main challenge in this research, since there's no previous study on this particular topic. Raff's critical gap model and logistic regression are selected to perform critical gap calibration for VISSIM simulation to ensure accurate results from simulation.

CHAPTER III

DATA COLLECTION

The data used in this research consists of two parts. The first part is the field data

collected from 30 unsignalized intersections across U.S., which is provided by the

NCHRP 3-91 project. This part of data was used for critical gap calibration in this

research. The second part is the simulation results from VISSIM simulation, which was

used to analyze the platoon impacts on left-turn operations.

Field Data

An extensive database was established for the NCHRP 3-91 project, Left-Turn

Accommodations at Unsignalized Intersections. 30 TWSC unsignalized intersections in

three states of United States (Texas, Arizona, and New York) were videotaped with DV

cameras, which allowed for measuring traffic volumes, gaps, gap acceptance behaviors,

left-turn delay and other important information in the field. Factors related to the

operations of these intersections were also recorded as part of this dataset, including

intersection geometry, speed limit and signal density. Out of the field data collected from

the 30 unsignalized intersections, three datasets were extracted and prepared for this

research. All the 30 unsignalized intersections were listed in the table on page 18 and 19.

The information related to the gap acceptance behavior of each individual major-

street left-turn (MSLT) vehicle was extracted into the gap acceptance dataset for gap

acceptance behavior study. The data was recorded and prepared by each gap presented to

the driver, each row corresponding to one gap. Part of the dataset of Intersection AZ-01

is as shown in Table 4, and the elements included in Table 4 are:

- Length of gaps presented to each vehicle (*gaptime* in Table 4),

- Gap acceptance decision (*response* in Table 4),

- Delay time in the queue (*queuetime* in Table 4),

- Delay time at the head of queue (*headtime* in Table 4),

- Turn time to cross approach and opposing lane (*turntime1*, *turntime2*, and

  turntime in Table 4), and

- Vehicle type.

Table 4 Partial Information of Gap Acceptance

Site	Vehicle No.	Gaptime (sec)	Response	Queuetime (sec)	Headtime (sec)	Turntime1 (sec)	Turntime2 (sec)	Turntime (sec)	Vehicle Type
AZ-01	1	0.87	Reject	0.15	4.06	1.42	2.75	4.17	VAN
AZ-01	1	1.00	Reject	0.15	4.06	1.42	2.75	4.17	VAN
AZ-01	1	32.00	Accept	0.15	4.06	1.42	2.75	4.17	VAN
AZ-01	2	16.34	Accept	0.14	0.75	1.07	2.45	3.52	SUV
AZ-01	3	1.34	Reject	0.14	6.12	1.49	3.27	4.76	CAR
AZ-01	3	2.00	Reject	0.14	6.12	1.49	3.27	4.76	CAR
AZ-01	3	2.00	Reject	0.14	6.12	1.49	3.27	4.76	CAR
AZ-01	3	31.34	Accept	0.14	6.12	1.49	3.27	4.76	CAR
AZ-01	4	17.69	Accept	0.14	2.10	0.89	2.78	3.67	CAR
AZ-01	5	8.22	Accept	0.16	0.88	1.36	2.50	3.86	SUV

In this research, the gap acceptance data was used to perform the critical gap

calibration with Raff's critical gap model and logistic regression model. Along with the

intersections characteristics in the table on page 18 and 19, the gap acceptance data

could be used to perform the detailed analysis of various factors that might affect critical gap. These factors included intersection geometry, vehicle type, speed, delay, etc.

The operational data of left-turn movement at unsingalized intersections were summarized in the second dataset for simulation calibration purpose. An example of the operational dataset is as shown in Table 5. The elements in the operational data table include:

- Start time of each 5-minite period recorded,

- Advancing, opposing, and left-turning volumes of each approach lane,

- Average delay time within each 5-min period (*queuetime* and *headtime* in Table 5), and

- Queue length.

The values of variables in Table 5 are the basis for deciding appropriate ranges for these variables in simulation scenario designing process. Besides, Table 5 contains the average MSLT delay within each 5-min period, which has been selected as the major measure of intersection operation levels. As one important step of the critical gap calibration, the delay outputs from VISSIM simulation using Raff's critical gap and logistic critical gap will be compared with this real-world delay to decide the better value for the critical gap of each intersection.

Table 5 Partial Information of Operation Data

Site	Start Time	Queuetime (sec)	Headtime (sec)	Queue Length	Major NB/WB Vol.			Major SB/EB Vol.		
					Left	Thru	Right	Left	Thru	Right
AZ-01	15:45:00	0.15	2.78	0	5	70	0	0	52	0
AZ-01	15:50:00	0.15	11.16	0	3	74	0	0	47	3
AZ-01	15:55:00	0.15	0.27	0	2	74	0	0	56	2
AZ-01	16:00:00	0.15	0.24	0	2	112	0	0	42	0
AZ-01	16:05:00	0.16	0.45	0	1	86	0	0	35	1
AZ-01	16:10:00	0.17	4.59	0	4	104	0	0	45	2
AZ-01	16:15:00	0.16	4.51	0	7	98	0	0	53	0
AZ-01	16:20:00	0.16	0.99	0	2	93	0	0	44	0
AZ-01	16:25:00	0.17	2.8	0	3	86	0	0	49	5
AZ-01	16:30:00	0.15	7.17	0	3	111	0	0	61	1

The last dataset, which summarizes the characteristics of each intersection, is partially shown in Table 6. Variables in this table include:

- Number of legs,

- Direction of the observed MSLT movement (Left-Turn Approach in Table 6),

- Number of segment lanes and left-turn lanes (*No. of LTL* in Table 6),

- Major Street name,

- Signal density,

- Number of lanes,

- Posted speed limit, and

- Median type and width.

The characteristics information contained in Table 6 was the basis for deciding the scenarios in simulation. The combinations of different characteristics provided in this

spreadsheet were coded in later simulation development. Besides, it was also necessary

for identifying and investigating the contributing factors to the critical gap.

Table 6 TWSC Intersection Characteristics

Site	Num of Legs	Left-Turn Approach	Major Name	Signal Density	LTL (1=Yes, 0=No)	Median Type	Median Width (ft)	Num of Lanes	Speed Limit (mph)
AZ-01	4 Legs	NB	32nd	1	1	TWLTL	10.00	2	40
AZ-02	3 Legs	NB	Tatum	0	1	LTL w/o Median	12.00	2	45
AZ-03	3 Legs	NB	Central	0	0	None	0.00	2	40
AZ-04	3 Legs	EB	Stanford	0	1	TWLTL	13.00	1	25
AZ-05	3 Legs	NB	Central	1	0	None	0.00	2	40
AZ-06	3 Legs	EB	Campbell	1	0	None	0.00	1	30
AZ-07	4 Legs	EB	CamelBack	2	0	None	0.00	1	25
AZ-08	3 Legs	NB	40th Street	1	1	TWLTL	11.00	2	35
AZ-09	4 Legs	NB	64th St	0	1	TWLTL	10.00	2	40
AZ-10	4 Legs	EB	Oak	1	0	None	0.00	1	25
AZ-11	3 Legs	NB	40th Street	0	1	TWLTL	9.00	1	35
AZ-12	3 Legs	EB	Indian School	1	1	TWLTL	11.00	2	40
AZ-13	4 Legs	EB	SR 84	0	1	LTL w/o Median	0.00	2	55
AZ-14	3 Legs	WB	Cornville	0	1	LTL w/Flush Median	1.00	2	50
AZ-15	3 Legs	EB	SR 347	0	1	LTL w/Flush Median	14.00	3	55
NY-01	3 Legs	WB	Jefferson	1	0	None	0.00	2	30
NY-02	3 Legs	NB	Hyland	1	0	Raised	3.67	2	35
NY-03	4 Legs	EB	Forest	1	0	None	0.00	1	30
NY-04	3 Legs	NB	South Avenue	1	1	LTL w/Raised Median	2.67	2	40
TX-01	3 Legs	SB	Wellborn	0	1	TWLTL	12.00	1	45
TX-02	4 Legs	EB	University	0	0	None	0.00	1	65

Table 6 Continued

Site	Num of Legs	Left-Turn Approach	Major Name	Signal Density	LTL (1=Yes, 0=No)	Median Type	Median Width (ft)	Num of Lanes	Speed Limit (mph)
TX-03	3 Legs	EB	Spring Cypress	1	0	None	0.00	2	30
TX-04	3 Legs	SB	Aldine West	0	0	None	0.00	2	35
TX-05	3 Legs	NB	Cypresswood	0	1	LTL w/ Raised Median	32.00	2	45
TX-06	3 Legs	NB	Wellborn	0	0	Flush	4.17	2	45
TX-07	3 Legs	WB	University	0	0	None	0.00	1	60
TX-08	4 Legs	WB	Shadow Creek	1	1	None	0.00	1	40
TX-09	4 Legs	NB	Fry	0	1	LTL w/ Raised Median	14.50	2	40
TX-10	4 Legs	EB	Broadway	0	1	TWLTL	13.00	2	40
TX-11	3 Legs	EB	Boonville	1	1	Raised	14.67	2	55

Simulation Results

The second part of the data used in this research was collected from the VISSIM simulation for the platoon impacts analysis. After the calibration work was finished, the VISSIM simulation was used to simulate different TWSC intersection scenarios with different types of platoons generated by upstream traffic signals. After the simulation work was finished, the left-turn delay at the downstream intersections was collected as the main measure of the operational well-being as well as some other useful data. An example of the simulation results of left-turn delay was shown in Table 7, whose elements include:

- Scenario number in the simulation,

- Platoon Time Ratio (see details in Chapter IV),

- Platoon Flow Ratio (see details in Chapter IV),

- Left-turn Delay within 1-hr period (see details in Chapter IV), and

- Total Delay within 1-hr period (see details in Chapter IV) at the intersection.

Table 7 Simulation Results

Scenario No.	Platoon Time Ratio (4veh/10s)	Platoon Flow Ratio (4veh/10s)	Platoon Time Ratio (5veh/10s)	Platoon Flow Ratio (5veh/10s)	Platoon Time Ratio (6veh/10s)	Platoon Flow Ratio (6veh/10s)	LT Delay (s/veh)	Total Delay (s/veh)
Out-1-1	0.18	2.36	0.09	2.76	0.05	3.08	5.2	0.7
Out-1-2	0.19	2.35	0.13	2.65	0.06	3.11	10.1	0.7
Out-1-3	0.22	2.22	0.09	2.70	0.05	2.98	5.3	0.7
Out-1-4	0.21	2.24	0.11	2.64	0.06	3.07	7.8	0.8
Out-1-5	0.21	2.26	0.12	2.64	0.07	3.00	6.3	0.7
Out-1-6	0.18	2.33	0.09	2.75	0.04	3.17	7.7	0.7
Out-1-7	0.20	2.27	0.09	2.79	0.06	3.04	7.7	0.7
Out-1-8	0.19	2.26	0.10	2.63	0.04	3.04	5.9	0.8
Out-1-9	0.23	2.09	0.10	2.52	0.05	2.80	12.4	0.9
Out-1-0	0.18	2.46	0.12	2.81	0.07	3.24	8.1	0.9

The simulations results table includes the left-turn and total delay data at the unsignalized intersections from simulation, also the values of the two platoon parameters. These data will be used to analyze the platoon impacts on left-turn delay and establish the relationship if the impacts do exist. Details of this analysis will be presented in Chapter IV.

CHAPTER IV

METHODOLOGY

The objective of this research is to develop a methodology for analyzing and estimating the platoon effects on the MSLT delay at TWSC intersections. The main idea is to use a microscopic simulation tool to simulate different platoon scenarios in opposing through traffic and applying regression models to capture the impacts of platoons on the delay of MSLT. The challenge in this research comes from the large number of factors affecting the platoons, which form complex combinations and make it difficult to analyze the platoon impacts. In order to solve this problem, two platoon variables were defined as a simplification of the complex platoon scenarios, making it practical to perform the analysis on platoon effects on delay. The structure of this research is illustrated in Figure 2.
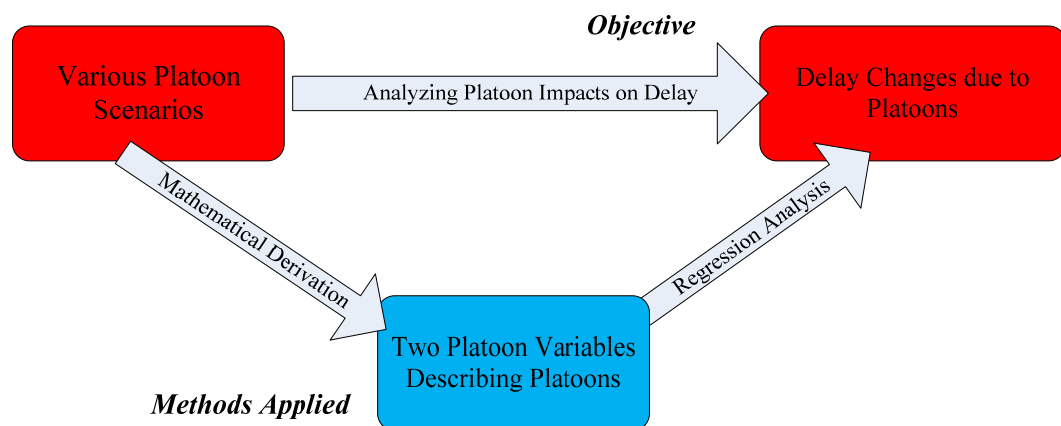

Figure 2 Structure of Research Methodology

This methodology includes: simulation model establishment and calibration, simulation scenarios development, platoon parameters derivation and calibration and delay adjustment with platoon effects. The steps are shown in Figure 3.

```
              ┌─────────────────────┐
              │  Platoon Scenarios  │
              │      Selection      │
              └─────────────────────┘
              ┌───────────┴──────────────────┐
              ▼                              ▼
   ┌─────────────────────┐        ┌─────────────────────┐
   │  Platoon Variables  │        │  Simulation Model   │
   │     Definition      │        │   Establishment &   │
   └─────────────────────┘        │     Calibration     │
              │                   └─────────────────────┘
              ▼                              ▼
   ┌─────────────────────┐        ┌─────────────────────┐
   │  Platoon Variables  │        │ Simulation Scenarios│
   │     Derivation      │        │     Development     │
   └─────────────────────┘        └─────────────────────┘
              │                              ▼
              │                   ┌─────────────────────┐
              │                   │   Simulation Data   │
              │                   │     Collection      │
              │                   └─────────────────────┘
              └──────────────┬───────────────┘
                             ▼
                  ┌─────────────────────┐
                  │  Platoon Variables  │
                  │     Calibration     │
                  └─────────────────────┘
                             ▼
                  ┌─────────────────────┐
                  │  Delay Adjustment   │
                  │ Factors Calculation │
                  └─────────────────────┘
                             ▼
                  ┌─────────────────────┐
                  │   Platoon Impacts   │
                  │     Evaluation      │
                  └─────────────────────┘
```
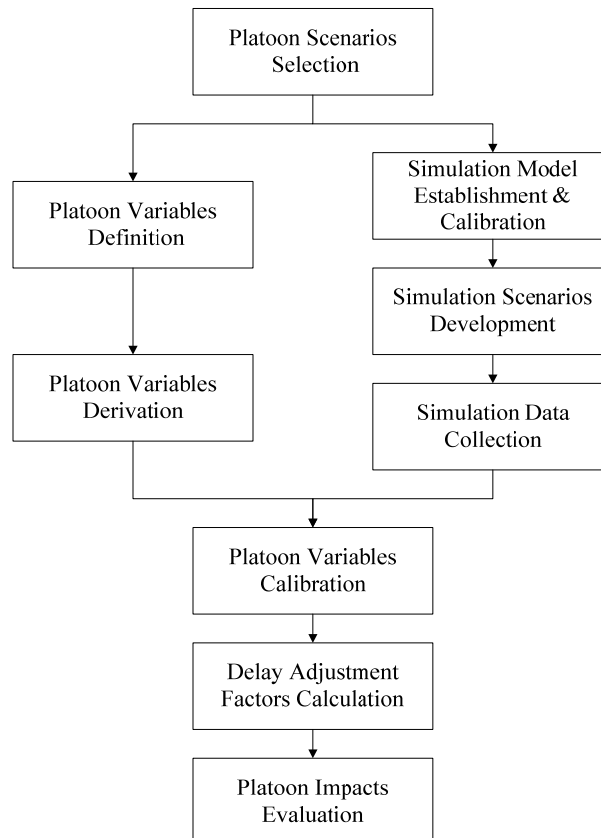
Figure 3 Steps in Research Methodology

Simulation Model Establishment and Calibration

VISSIM, developed by PTV AG, Karlsruhe, was selected as the platform for performing the simulation work in this research [*23*]. VISSIM is a leading microscopic simulation program for multi-modal traffic flow modeling. It provides high-accuracy

traffic simulation through allowing users to adopt detailed input values and tune a large number of parameters in the model.

Two-way stop-control (TWSC) unsignalized intersections were coded and simulated in VISSIM to fulfill the goal of this research. The intersections simulated in this research are four-leg intersections, with two major streets and two minor streets. The MSLT movement, which is the focus of this research, is controlled by a gap acceptance model established through a function called "Priority Rule" in VISSIM. "Priority Rule" allows users to specify values for the critical gap. Minor-street movements are controlled by stop signs.

The idea of gap acceptance model of left-turn movement at unsignalized intersection is illustrated through the example in Figure 4. In Figure 4, a group of MSLT vehicles are waiting to take a permissive left-turn at the unsignalized intersection, which is denoted by the red arrow. The left-turn vehicles have to wait for a sufficiently large gap among opposing through traffic to make a safe left-turn. The gap is also shown in Figure 4 by the blue arrow, which is defined as the time headway between two consecutive vehicles. The gap is the most important data in the process of simulation parameter calibration. The gap data, intersection characteristics data and other related information used in this research are provided by Dr. Kay Fitzpatrick. An introduction to the datasets has been made in Chapter III.
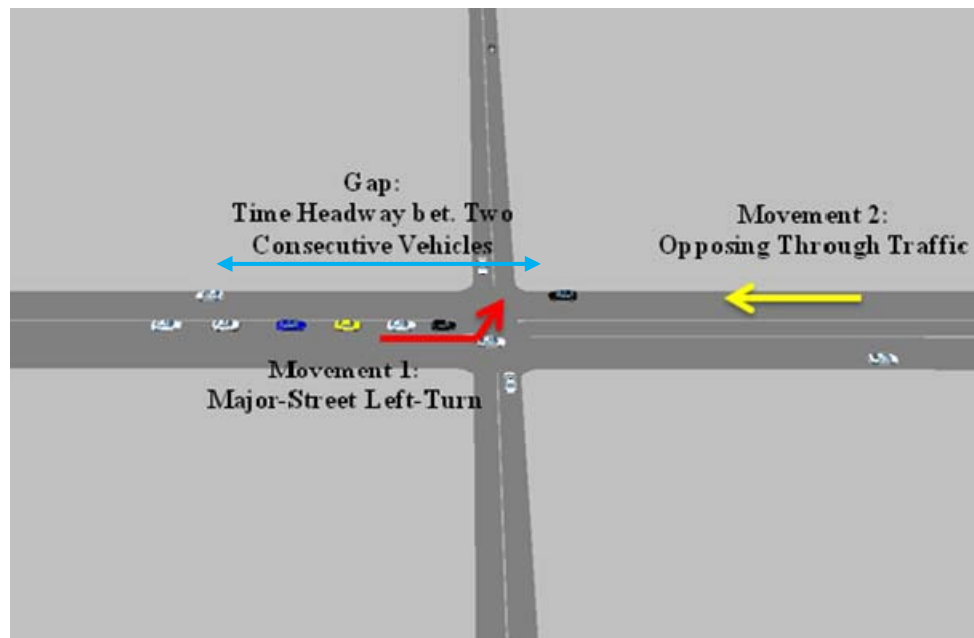
Figure 4 Chart of Gap Acceptance Model

Two methods were employed to perform the critical gap calibration and analysis of various factors' effects on the critical gaps: Raff's critical gap model, and logistic regression model.

Raff's Critical Gap Model

Raff's method is the most commonly used method for estimating critical gaps. The definition is that critical gap value is the length of gap whose probability of being accepted equals its probability of being rejected. This method can also be interpreted as the cumulative probability where functions $1 - F_r(t)$ and $F_a(t)$ intercept as shown in Equation 3.

$$1 - F_r(t) = F_a(t) \tag{3}$$

where $F_a(t) =$ cumulative distribution function for the accepted gaps,

$F_r(t) =$ cumulative distribution function for the rejected gaps.

To calibrate the critical gap with Raff's method in this research, the gap acceptance data collected for NCHRP 3-91 project was used. The dataset's form was shown in Table 4, which included information of length of gaps, gap acceptance decision, delay time in the queue, delay time at the head of queue, turn time to cross approach and opposing lane. The whole dataset was divided into 30 sub-datasets by intersection, and at each individual intersection, the gaps being accepted by drivers and that being rejected were separated. The statistics programming software R was used to calculate $1 - F_r(t)$ and $F_a(t)$, which are two essential variables for exploring the Raff's critical gap at each intersection.

AZ-01 Raff's Critical Gap
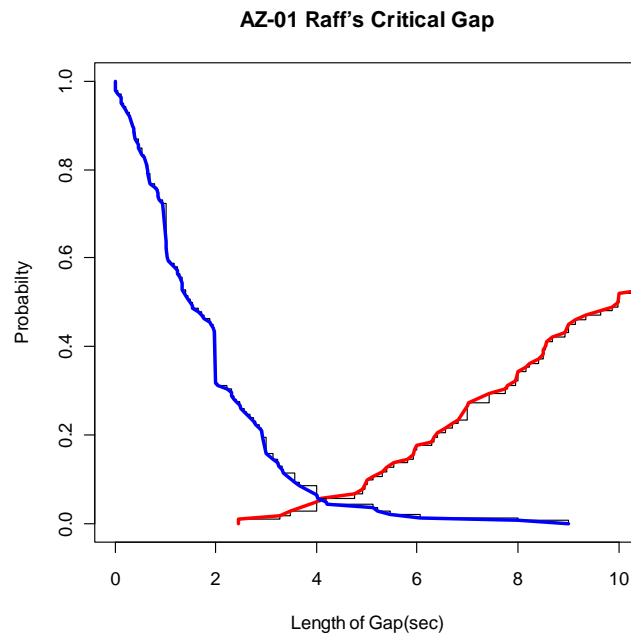
Figure 5 AZ-01 Raff's Critical Gap

As an example, the Raff's Critical Gap Plot is shown in Figure 5. The cumulative probability function was plotted for $F_a(t)$ and $1 - F_r(t)$ for the intersection "Arizona-01". The red line and the blue line denote the cumulative probability function of $F_a(t)$ and $1 - F_r(t)$ respectively based on the gap data. The gap length of the point where two lines intersected was considered as the critical gap from this method. In this example, the critical gap for intersection "Arizona-01" was 4.1 second. The same operation was repeated for all 30 unsignalized intersections to calculate the Raff's critical gap.

Logistic Regression Model

The second method used in this research to calibrate the critical gap is logistic regression model. Unlike regular dependent variables in linear regressions, the dependent variable in gap acceptance model is based on a series of "accept"/ "reject" responses [*24*]. Ideally such responses follow a binomial distribution and the appropriate model is the logistic regression model. Logistic regression was applied to examine the factors that potentially affect drivers' gap acceptance behaviors and also to generate a regression model for calculating the critical gap based on the field data.

The first step was to establish a gap acceptance model to calculate the probability that drivers accept a gap, taking into consideration the factors that may affect the critical gaps, including the length of gap, intersection geometry, posted speed limit, and waiting time at the head of the queue. The gap acceptance dataset shown in Table 4 was grouped into sub-datasets by intersection, and the gap acceptance probability model was established for each individual unsignalized intersection.

For each intersection, probability of accepting a gap, the dependent variable, in a logistic regression was converted to the log of the odds ratio, as shown in Equation 4. This is known as the logit. This is the dependent variable against which independent variables are regressed.

$$logit = \log\left(\frac{\theta}{1-\theta}\right) \tag{4}$$

where θ = the probability of "accept",

$$\left(\frac{\theta}{1-\theta}\right) = \text{the ratio of probability of "accept" to that of "reject".}$$

Therefore, the logistic regression for calculating the probability of a particular gap being accepted can be established in the format in Equation 5. The terms of $\beta_i x_i$ are introduced into the logit equation to account for the contributing factors that may have impacts on the gap acceptance behavior of drivers. The only contributing factor in this research is the length of gaps presented to each vehicle. Other factors including delay time in the queue, delay time at the head of queue, turn time to cross approach and opposing lane are not considered in this research because 1) length of the gap is the dominating factor that affects gap acceptance behavior, and 2) other factors cannot be reflected in the simulation. Equation 6 is the form of the model used to perform logistic regression for each intersection.

$$logit = \log\left(\frac{\theta}{1-\theta}\right) = \beta_0 + \beta_1 x_1 + \beta_2 x_2 + ... + \beta_i x_i \tag{5}$$

$$logit = \log\left(\frac{\theta}{1-\theta}\right) = \beta_0 + \beta_1 x_{gap} \tag{6}$$

where β_0 = intercept in the logistic regression model,

β_i = coefficient for x_i in the logistic regression model,

x_i = an independent variable in the logistic regression model, and

x_{gap} = independent variable of length of the gap.

Based on the field gap data, the parameters in Equation 6 were calibrated using maximum likelihood estimation with statistical tools. Once the logistic regression model was established based, the probability of being accepted or rejected could be calculated using Equation 7.

$$\theta = \frac{1}{1+\exp(-\{\beta_0 + \beta_1 x_{gap}\})} \tag{7}$$

The second step of calibrating the critical gap with logistic regression model was to define and calculate the critical gap for each intersection. In this research, the critical gap was defined as the gap for which the probability of accepting it according to the logistic regression model is equal to rejecting it, i.e. if $\theta = 1 - \theta = 0.5$, the gap length was considered as the critical gap. This calibration process was repeated for all the 30 intersections in the dataset.

Comparison of the Two Methods

Two sets of critical gaps were calibrated for all the 30 intersections with Raff's model and logistic regression model respectively. Both of the two sets of critical gaps were tried in the VISSIM simulation and the delay was collected from the simulation in periods of 5 minutes for around 100 MSLT vehicles. Squared deviation between the simulated delay and the field data was calculated to compare the two sets of critical gaps and decide which one matches the real-world data better.

Table 8 Comparison of Raff's and Logistic Method

Time Bin	LT Delay (10 run average)		LT Delay from	Squared Deviance (vs. Field Data)	
(5 min)	Using Raff's Critical Gap	Using Logistic Critical Gap	Field Data	Using Raff's Critical Gap	Using Logistic Critical Gap
1	2.17	3.05	2.93	0.58	0.01
2	2.06	2.05	11.32	85.75	85.93
3	4.28	4.64	0.42	14.90	17.81
4	2.22	2.46	0.39	3.35	4.28
5	0.38	0.38	0.61	0.05	0.05
6	1.53	1.65	4.76	10.43	9.67
7	2.67	3.45	4.67	4.00	1.49
8	3.12	3.56	1.15	3.88	5.81
9	4.56	4.56	2.97	2.53	2.53
10	2.72	3.66	7.32	21.16	13.40
11	4.06	4.53	1.77	5.24	7.62
12	2.72	2.99	1.18	2.37	3.28
13	4.61	5.14	0.94	13.47	17.64
14	2.81	3.03	2.57	0.06	0.21
15	2.1	2.28	4.37	5.15	4.37
16	1.57	2.44	3.81	5.02	1.88
17	2.69	2.74	3.4	0.50	0.44
18	1.6	2.19	4.16	6.55	3.88
19	1.8	1.95	5.21	11.63	10.63
20	2.61	2.79	2.34	0.07	0.20
21	3.48	3.89	7.75	18.23	14.90
22	2.5	2.66	2.75	0.06	0.01
23	2.73	3.07	24.12	457.53	443.10
24	3.34	3.86	4.35	1.02	0.24
25	2.77	3.36	4.63	3.46	1.61
26	2.4	2.76	3.5	1.21	0.55
Total of Squared Deviation				678.22	651.53

As illustrated by the example of Intersection AZ-01 in Table 8, the critical gap with smaller total squared deviation was selected as the final critical gap for this particular intersection. The Raff's critical gap calibrated for AZ-01 is 4.1 seconds and logistic critical gap is 4.5 seconds. Both critical gaps were used to calibrate the

simulation and the left-turn delay results were collected. The deviation of left-turn delay values from VISSIM simulation vs. the field delay data were calculated in this example, which served as the measure for final decision. Critical gap that gave smaller squared deviance of left-turn delay between the simulated results and real-world data was chosen as the final critical gap. In this example, Raff's critical gap gives a squared deviance value of 678.22 while logistic critical gap gives 651.53, which means the final critical gap for AZ-01 will be the 4.5-second logistic critical gap.

The selection of critical gap will be performed for all the 30 intersections and the final set of critical gaps will be further investigated in terms of contributing factors that may influence the critical gap at an unsignalized intersection. T-test will be applied to find out the factor that have impacts on the critical gap and a specific table of critical gaps will be recommended for the simulation of platooning scenarios.

Simulation Scenarios Development

First, four intersection categories were defined: two-lane with a left-turn lane (LTL), two-lane without a LTL, four-lane with a LTL and four-lane without a LTL.

Second, for each intersection category, a set of operational scenarios was coded, each scenario representing a certain combination of approach volume, opposing volume, the observed left-turn volume, and speed limit. When generating these scenarios, advancing and opposing volumes were varied between 400 and 800 Vehicles per hour per lane(vphpl) at an increment of 200 vphpl and left-turn volume was varied between

20 and 140 vphpl at an increment of 40 vphpl. Speed limits included 30 mph, 40 mph, and 50 mph.

Finally, for each scenario, a fix-timed traffic signal was installed upstream from the observed unsignalized intersection to generate platoon arrivals for MSLT movement at the downstream intersection. A set of 27 upstream traffic signals were coded for each scenario to generate platoons of various intensities. The traffics signals were set up based on combinations of distance to the downstream intersection, with cycle length and green-red split as shown in Table 9.

Table 9 One Set of Upstream Traffic Signals

Distance (ft)	Cycle Length (sec)	Green-red Split		
	60	40/20	30/30	20/40
600	90	60/30	45/45	30/60
	120	80/40	60/60	40/80
	60	40/20	30/30	20/40
1500	90	60/30	45/45	30/60
	120	80/40	60/60	40/80
	60	40/20	30/30	20/40
2400	90	60/30	45/45	30/60
	120	80/40	60/60	40/80

A typical Simulation Scenario of unsignalized intersection simulated in this research is shown in Figure 6. The red arrow denotes MSLT traffic and the black arrow stands for opposing through traffic coming from upstream signalized intersection.
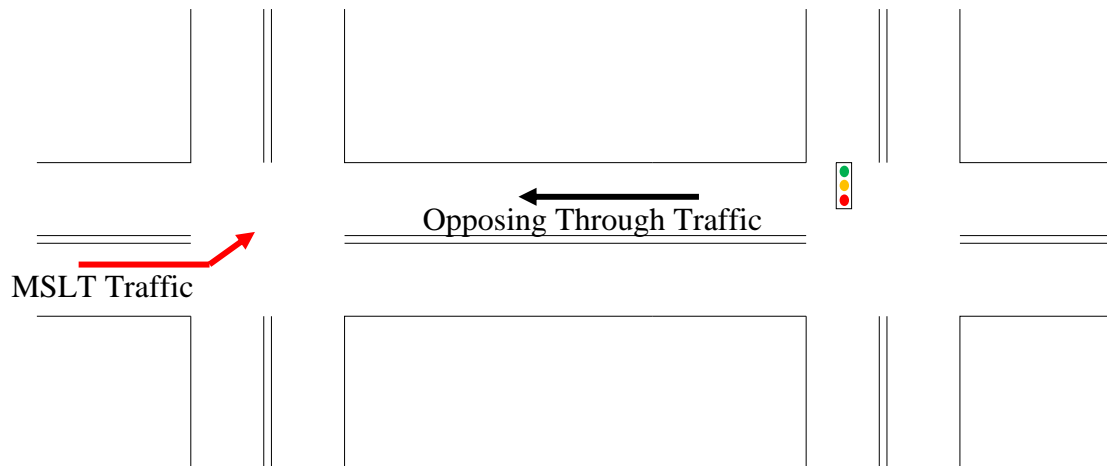
Figure 6 Simulation Scenario Example

Each scenario's simulation lasted for 3600 seconds and was repeated ten times with different random seeds in VISSIM, with the ten-run average as the final result. The output from all these runs formed a comprehensive dataset, among which control delay (s/veh) was used as the major performance measure of left-turn operation at each scenario. The number of arrivals of opposing through traffic within each 10-second time interval during a 1-hour period was also recorded to calculate platoon related variables in later sections. Some other related variables were also calculated and added into the dataset if they are necessary for the platoon impacts analysis.

Platoon Variables Definition and Calibration

A number of factors affect the platoon arrivals from an upstream signalized intersection to a downstream unsignalized intersection. These factors include hourly through traffic volume, traffic signal timing plan (cycle length and green-red split), the arrival times of through vehicles to the signalized intersection with respect to its signal state, the level of platoon dispersion occurring between the signalized intersection and the downstream unsignalized intersection. This is a fairly long list, which makes it very difficult to analyze all the combinations of these factors while identifying patterns, as well as being able to present the results in a meaningful way.

As mentioned in the literature part, for analysis of platoon effects at signalized intersection, the variable of platoon ratio (R_p) was defined to describe the platoons at signalized intersection. In order to simplify the analysis and better present the results, similar idea was brought up for this research. Due to the complexity of platoons at unsignalized intersection, two variables (the platoon time ratio and the platoon flow ratio) were defined for describing the platoon arrivals, and they can be calculated using a platoon dispersion model.

Platoon time ratio (R_{pt}), is defined as the ratio of the time with platoons in opposing through traffic to the total time within the period of one hour. Platoon flow ratio (R_{pf}), is defined as the ratio of average flow rate in the time with platoons to the overall averaged flow rate within in the period of one hour. Two sets of the same variables (but from different sources) were involved in this research.

The first set of platoon variables was derived using a platoon dispersion model, and the two variables were defined as platoon time ratio from derivation (R^D_{pt}) and platoon flow ratio from derivation (R^D_{pf}). The purpose of the first set of platoon variables was to deal with the huge number of combinations of factors that affected platoons, which combined all the factors and describe the platoons with simply two variables.

The platoon time ratio of the first set of platoon variables (R^D_{pt}) could be derived with a platoon dispersion model. The derivation was found in literature (Bonnesson, 1996), which can be summarized as:

$$t_p = \begin{cases} g_q - \dfrac{\ln[(1-\dfrac{v_{o,\min}}{sf})(\dfrac{v_{o,\max}-v_u f}{v_{o,\min}-v_u f})]}{\ln(1-F)} & sf > v_{o,\min} \\ 0.0 & sf < v_{o,\min} \end{cases} \tag{8}$$

$$R^D_{pt} = \frac{t_p}{C} \tag{9}$$

with

$$v_{o,\max} = \frac{v_{o,p}}{n_o} f[1-(1-F)^{g_q}] \tag{10}$$

$$F = \frac{1}{1+\alpha\beta t_a} \tag{11}$$

$$g_q = \frac{(C-g)v_u}{s-v_u} \tag{12}$$

$$t_a = \frac{D}{S} \tag{13}$$

$$f = 1 - \frac{\sum v_{in}}{v_c} \geq 0.0 \qquad (14)$$

where

$R^D_{pt} =$ platoon time ratio from derivation;

$f =$ portion of opposing stream that originated as a through movement at the upstream signalized intersection;

$F =$ smoothing factor;

$g_q =$ effective green time required to discharge the stopped queue of the opposing through movement at the upstream signalized intersection (sec);

$v_{o,\max} =$ maximum flow rate in the opposing traffic (vpspl);

$v_{o,\min} =$ user–defined minimum flow rate for platoons in the opposing traffic (vpspl);

$\alpha =$ platoon dispersion factor;

$\beta =$ ratio of travel time of lead platoon vehicle to average platoon vehicle (= 0.80);

$t_a =$ average travel time from the upstream signalized intersection to the subject movement (sec);

$t_p =$ time with platoons within one cycle (sec);

$C =$ cycle length of the upstream signalized intersection (sec);

$g =$ effective green time for the opposing through movement at the upstream intersection (sec);

$v_u =$ flow rate of the opposing through movement at the upstream intersection (vpspl);

$D =$ distance between the upstream signalized intersection and the subject movement (m);

$S =$ average running speed of the platoon (m/sec);

$s =$ saturation flow rate of the conflicting through movement at the upstream signalized intersection

$n_o =$ number of lanes serving the opposing through traffic;

$v_{in} =$ flow rate of all movements that enter the arterial and travel in the same direction as the opposing through movement;

$v_{o,p} =$ flow rate of the opposing traffic during the platoon period (vps);

$v_{o,n} =$ flow rate of the opposing traffic during the non-platoon period (vps); and

$v_o =$ average flow rate of the opposing traffic (vps).

The platoon flow ratio of the first set (R^D_{pf}) was derived and summarized in this research in Equation 15 and 16. Detailed derivation process was documented in Appendix A.

$$n_{a,p} = sf(g_q - t_b) + v_u f(t_e - g_q) + \frac{1 - (1-F)^{g^q} + (1 - \frac{1}{sf}) v_{o,min} - v_{o,max}}{\ln(1-F)} \quad (15)$$

$$R^D{}_{pf} = \frac{n_{a,p}}{v_o t_p} \quad (16)$$

with

$$t_b = \frac{\ln(1 - \frac{v_{o,min}}{sf})}{\ln(1-F)} \quad (17)$$

$$t_e = g_q + \frac{\ln(\frac{v_{o,min} - v_u f}{v_{o,max} - v_u f})}{\ln(1-F)} \quad (18)$$

where

$R^D{}_{pf} =$ platoon flow ratio;
$n_{a,p} =$ number of arrivals in platoon intervals;
$t_b =$ the beginning time of the platoon; and
$t_e =$ the ending time of the platoon.

The second set was calculated from the platoon arrival data collected from the

simulation, and the two variables were defined as platoon time ratio from simulation

($R^S{}_{pt}$) and platoon flow ratio from simulation ($R^S{}_{pf}$). The second set of platoon variables

was used directly in the analysis of platoon impacts on delay, and was also used as the

yardstick to calibrate the derivation equations for the first set of platoon variables.

As mentioned earlier, the number of arrivals of opposing through traffic within

each 10-second time interval during a 1-hour period was recorded for this calculation. In

this research, the intervals with more than 3 arrivals (3vehicles/10seconds) at two-lane

intersections were defined as the platoon intervals, while 5 arrivals

(5vehicles/10seconds) was the critical value for four-lane intersections.

The two platoon variables of the second set (R^S_{pt} and R^S_{pf}), can be calculated

based on the data collected from simulation using the following equations:

$$R^S_{pt} = \frac{10\sec \times n_{i,p}}{10\sec \times n_i} = \frac{10\sec \times n_{i,p}}{3600\sec} = \frac{n_{i,p}}{360} \tag{19}$$

$$R^S_{pf} = v_{o,p}/v_o = \frac{n_{a,p}}{10\sec \times n_{i,p}} / \frac{n_a}{3600\sec} = \frac{n_{a,p}}{n_a R^S_{pt}} \tag{20}$$

where

R^S_{pt} = platoon time ratio from simulation;
R^S_{pf} = platoon flow ratio from simulation;
$n_{i,p}$ = number of platoon intervals ;
n_i = number of all intervals within 1 hour;
$n_{a,p}$ = number of arrivals in platoon intervals; and
n_a = number of all arrivals within 1 hour.

Both sets of platoon variables are involved in this research to analyze the platoon

impacts on MSLT delay. The purpose of the first set of platoon variables (R^D_{pt} and R^D_{pf}

) is to combine all the factors that affected platoons and describe the platoons in a simple

way. The second set of platoon variables (R^S_{pt} and R^S_{pf}) is used directly for the analysis

of platoon impacts on delay and for the calibration of the first set.

However, the mathematical derivations do not necessarily match the simulation

results perfectly, since the VISSIM simulation tool does not adopt the same platoon

dispersion model with which the mathematical derivation is performed. Even during a

period of platoon arrival, the headway between vehicles and arrival flow rate may

fluctuate in the real-world and in micro simulation. A practical method that combines the

two sets of platoon variables was proposed in this research, one that could both handle

the large number of combinations of related factors, and serve as the basis for platoon

impacts on MSLT delay.

Therefore, further calibration of the derivation equation with the data collected in

the simulation is needed before use. A linear regression model was developed to identify

the relationship between the variable values from derivation and those from simulation.

This calibrated regression model can then be used for further platoon impacts analysis

from given scenarios.

Delay Adjustment with Platoon Effects

After using the two platoon variables to describe platoon arrivals, the next step is

to look into how the platoon arrivals in opposing through traffic affect the delay of

MSLT movement at TWSC intersections. In order to quantify the platoon arrivals'

impacts, the delay adjustment factor (F_{da}) was defined. F_{da} was defined as the ratio of

left-turn delay under platoon arrivals in opposing through traffic to that under random

arrivals. The F_{da} is a measure of how much the platoon arrivals are changing the left-turn

delay from random-arriving situations. In this research, F_{da} was calculated for each 1-

hour/3600-sec period based on the delay data collected from the simulation.

$$F_{da} = \frac{d_p}{d_r}$$
(21)

where

      d_p = MSLT delay under platooning arrivals in each 3600-sec scenario, and
      d_r = MSLT delay under random arrivals in each 3600-sec scenario.

    If some relationship between the two platoon variables (R^S_{pt} and R^S_{pf}) and the

delay adjustment factors (F_{da}) can be found, the impacts of platoon arrivals in opposing

through traffic will be evident. Linear or other forms of regression models could be

employed to establish the relationship between the two platoon variables and F_{da}.

CHAPTER V

RESULTS

Critical Gap Calibration Results

Raff's critical gap model and logistic regression model were adopted in this

research to calibrate the critical gaps of the 30 intersections involved in the dataset. As

mentioned in Chapter IV, the calibration was performed by each individual intersection.

For the Raff's model, the curves of a particular gap being accepted and rejected

were plotted on the same chart and the intercepting point of the two curves is the critical

gap for the intersection. One example is shown in Figure 5 and the complete collection is

in Appendix B.

For the logistic regression model, the gap value making the probability of the gap

equal to 0.5 is defined as the critical gap. The probability model was established in the

form of logistic regression, setting driver response as the dependent variable and length

of the gap as the independent variable. The collection of results is shown in Appendix C.

The two sets of critical gaps from Raff's critical gap model and logistic

regression model were tested in the VSSIM simulation in order to decide which critical

gap of the two yielded simulation closer to the field data. The critical gap with smaller

squared deviation of delay from the field delay data was chosen as the final critical gap

for each intersection. The Raff's critical gaps, logistic regression critical gaps and the

squared deviation of delay between real-data delay and simulation delay using respective

critical gap were summarized in Table 10. The critical gap that led to a better fit of the

real-world was chosen as the final critical gap for each intersection. See detailed process in Table 8 and the whole collection in Table 10.

Also observed from the comparison of the two models was that Raff's model and logistic model calibration did not show significant difference in total squared deviation of left-turn delay. Through this comparison, Raff's model was actually preferred, because logistic regression was much more sophisticated model but giving similar results, which should be avoided when choosing the calibration model. Therefore, for future calibration work, Raff's model was recommended unless other complicated model could yield results of significantly better quality.

Table 10 Critical Gaps from Raff's and Logistic Regression Model

Site	Raff's Critical Gap	Squared Deviation of Delay	Logistic Critical Gap	Squared Deviation of Delay	Final Critical Gaps
AZ-01	4.1	678.217	4.5	651.534	4.5
AZ-02	3.4	88.9696	2.2	112.041	3.4
AZ-03	3.9	329.010	3.6	340.171	3.9
AZ-04	6.6	364.812	6.2	385.405	6.6
AZ-05	4.0	1416.17	4.5	1364.870	4.5
AZ-06	4.4	333.203	4.4	333.203	4.4
AZ-07	6.4	116.499	5.4	107.503	5.4
AZ-08	4.5	174.134	4.6	163.675	4.6
AZ-09	4.9	594.788	4.9	594.788	4.9
AZ-10	4.9	26.272	1.8	17.376	4.9
AZ-11	4.8	1982.000	5.4	1892.710	5.4
AZ-12	4.1	1134.570	5.6	1216.270	4.1
AZ-13	7.8	466.196	6.2	471.715	7.8
AZ-14	4.7	--	4.9	--	4.8
AZ-15	5.2	42.522	4.9	43.105	5.2
NY-01	3.9	742.247	3.8	718.533	3.8
NY-02	3.3	1744.750	4.5	1243.390	4.5
NY-03	4.0	397.900	4.3	397.739	4.3
NY-04	4.9	--	5.6	--	5.25
TX-01	4.6	898.590	4.8	838.333	4.8
TX-02	6.0	24.590	5.0	42.601	6
TX-03	4.2	744.586	5.2	423.022	5.2
TX-04	3.9	148.921	3.3	162.899	3.9
TX-05	6.0	330.947	4.7	487.201	6
TX-06	5.3	127.124	4.9	147.801	5.3
TX-07	5.8	426.190	5.7	430.127	5.8
TX-08	4.4	583.957	4.7	541.430	4.7
TX-09	4.2	3071.590	5.6	3214.590	4.2
TX-10	3.1	1026.030	4.7	838.392	4.7
TX-11	4.5	179.974	4.8	152.603	4.8

Based on the final critical gaps established in Table 10, a further analysis on critical gaps in terms of the geometric and operational characteristics of the intersection was performed to get more accurate critical gap for simulation. The final critical gaps and intersection factors were summarized in Table 11. The factors that potentially affect the critical gap values were chosen from Table 6 for the analysis. The factors included:

- Number of legs (*No. of Legs* in Table 11),

- Number of left-turn lane (*No. of LTL* in Table 11),

- Number of lanes (*No. of Lanes* in Table 11),

- Median presence,

- Posted speed limits, and

- Average waiting time at the head of the queue for left-turn at each intersection

  (*Avg. Waiting Time* in Table 11).

Table 11 Final Critical Gap Values for Each Intersection

Site	Final Gaps (sec)	No. of Legs	No. of LTL	No. Lanes	Median Presence	Median Width (ft)	Speed Limit (mph)	Avg Waiting Time (sec)
AZ-01	4.5	4	1	2	1	10	40	3.66
AZ-02	3.4	3	1	2	1	12	45	1.95
AZ-03	3.9	3	0	2	0	0	40	2.75
AZ-04	6.6	3	1	1	1	13	25	3.45
AZ-05	4.5	3	0	2	0	0	40	4.94
AZ-06	4.4	3	0	1	0	0	30	1.61
AZ-07	5.4	4	0	1	0	0	25	1.1
AZ-08	4.6	3	1	2	1	11	35	3.36
AZ-09	4.9	4	1	2	1	10	40	3.68
AZ-10	4.9	4	0	1	0	0	25	0.6
AZ-11	5.4	3	1	1	1	9	35	5.02
AZ-12	4.1	3	1	2	1	11	40	8.27
AZ-13	7.8	4	1	2	0	0	55	1.66
AZ-14	4.8	3	1	2	1	1	50	4.08
AZ-15	5.2	3	1	2	1	14	55	2.7
NY-01	3.8	3	0	2	0	0	30	4.42
NY-02	4.5	3	0	2	1	4	35	7.67
NY-03	4.3	4	0	1	0	0	30	4.96
NY-04	5.25	3	1	2	1	3	40	6.81
TX-01	4.8	3	1	1	1	12	45	5.2
TX-02	6	4	0	1	0	0	65	1.49
TX-03	5.2	3	0	2	0	0	30	5.92
TX-04	3.9	3	0	2	0	0	35	1.64
TX-05	6	3	1	2	1	32	45	3.31
TX-06	5.3	3	0	2	1	4	45	3.44
TX-07	5.8	3	0	1	0	0	60	2.44
TX-08	4.7	4	1	1	0	0	40	2.8
TX-09	4.2	4	1	2	1	15	40	8.23
TX-10	4.7	4	1	2	1	13	40	6.92
TX-11	4.8	3	1	2	1	15	55	3.72

The overall averaged critical gap for left-turn movement at TWSC intersections is 4.9 second, calculated by averaging all the critical gaps of 30 intersections. This critical gap is larger than the 4.1 sec critical gap for left-turn movement that recommended in the 2000 HCM. It is probably due to the low traffic volume at unsignalized intersections in this NCHRP project, which needs further exploration to confirm it. Furthermore, in order to identify the factors that have impacts on critical gaps of left-turn movement, t-test was employed to compare the different critical gaps between groups divided by potential factors. The t-test results were summarized in Table 12.

Table 12 T Test for Factors Related to Critical Gaps

Factor	No. of Legs	No. of LTL	No. of Lanes	Median Presence	Speed Limit
Group Means	3-Leg:4.8 4-Leg:5.1	0-LTL:4.8 1-LTL:5.0	2-Lane: 5.2 4-Lane: 4.8	0-Median: 5.0 1-Median: 4.9	Low: 4.7 High: 5.4
t value	-0.852	-0.888	1.463	0.407	-1.798
df	14.21	27.941	22.447	19.708	12.098
p value	0.204	0.191	0.079	0.237	0.049
90% CI	(-Inf, 0.189)	(-Inf, 0.135)	(0.045, Inf)	(-0.387, Inf)	(-Inf, -0.173)

*Note: For Speed Limit, "Low" means lower or equal to 40 mph, while "High" is higher than 40 mph.

From Table 12, two factors were found to have impacts on critical gap values. Speed limit and number of lanes were found to cause significant differences between critical gaps of different groups with 90% confidence. The impacts on critical gap values by the two factors were summarized as below:

- The critical gap of two-lane intersections is significantly larger than that of four-lane intersections with 90% confidence.

- Intersections with higher posted speed limit tend to have larger critical gaps than those with lower speed limit.

Therefore, critical gaps were proposed in terms of number of lanes and posted speed limit of the intersections. The updated categorical critical gap values were shown in Table 13. There are two reasons might lead to the fact that two-lane intersection has larger critical gap than that of four-lane: first, two-lane roads typically have much lower traffic volume, therefore left-turn drivers are able to take generally larger gaps; second, for a left-turn drivers, four-lane roads have two opposing lanes which decreases the chances of having large gaps, lowing drivers' expectation and making them more aggressive in gap acceptance. When it comes to speed limits, the higher the speed is, the higher risk there is, therefore larger critical gap has been adopted in high speed intersection due to the safety concern.

Table 13 Recommended Critical Gap Values

Number of Lanes	Final Critical Gap(sec)	
	Low Speed	High Speed
2	5.1	5.5
4	4.5	5.3

Calibration of Platoon Variables from Derivation

As mentioned in Chapter IV, the mathematical derivations of the two platoon

ratios need to be further calibrated based on the simulation results before being used to

provide platoon variables for future analysis.

In order to perform the calibration of platoon variables from derivation, a dataset

in the form of Table 14 was prepared (Only the first 5 rows are shown). It included the

characteristics of the intersection, as well as platoon variables extracted from the

simulation and those from the mathematical derivations. R^S_{pt} and R^S_{pf} are the platoon

time ratio and platoon flow ratio calculated based on the simulation results using

Equation 19 and 20; R^D_{pt} and R^D_{pf} are calculated from Equation 9 and 16 as the platoon

time ratio and platoon flow ratio from derivation.

Table 14 Platoon Variables for Four-Lane TWSC Intersections

Speed (mph)	Distance (ft)	Approach Volume (vphpl)	Opposing Volume (vphpl)	LT Volume (vphpl)	Red Time Portion	Signal Cycle (sec)	R^S_{pt}	R^S_{pf}	R^D_{pt}	R^D_{pf}
30	600	400	400	20	0.33	60	0.13	2.90	0.10	3.73
30	600	400	400	20	0.50	60	0.17	3.10	0.16	3.97
30	600	400	400	20	0.67	60	0.20	3.39	0.21	4.09
30	600	400	400	20	0.33	90	0.15	2.97	0.10	3.97
30	600	400	400	20	0.50	90	0.21	3.33	0.16	4.14

The calibration for platoon variables from derivation is based on the values

calculated from the simulation results. The correlation between the derived platoon

ratios and the platoon ratios collected from the simulation needs to be established for the

calibration. The linear regression model was applied to identify the correlation. The

regression results of four-lane TWSC intersections were shown in Table 15 for Platoon

Time Ratio and Platoon Flow Ratio respectively.

Table 15 Relationships between Simulated and Derived Parameters for Four-Lane TWSC Intersection

R^S_{pt}					R^S_{pf}				
Estimate	Std.	Error	t value	Pr(>|t|)	Estimate	Std.	Error	t value	Pr(>|t|)
(Intercept) 0.180	0.004	48.36	<2e-16 ***		(Intercept) 0.745	0.032	22.98	<2e-16 ***	
R^D_{pt} 0.399	0.010	39.27	<2e-16 ***		R^D_{pf} 0.685	0.011	61.59	<2e-16 ***	
Residual standard error:					Residual standard error:				
0.06052 on 970 degrees of freedom					0.2773 on 970 degrees of freedom				
Multiple R-squared: 0.6139					Multiple R-squared: 0.7964				
Adjusted R-squared: 0.6135					Adjusted R-squared: 0.7962				
F-statistic: 1542 on 1 and 970 DF					F-statistic: 3794 on 1 and 970 DF				
p-value: < 2.2e-16					p-value: < 2.2e-16				
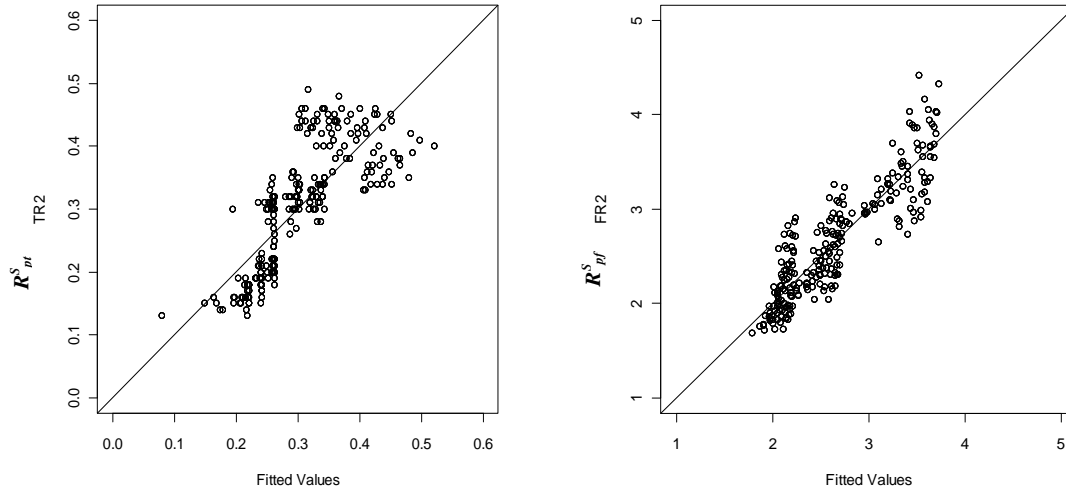
Figure 7 Simulated Platoon Variables vs. Fitted Values for Four-Lane TWSC Intersections

For both platoon time ratio and platoon flow ratio, the regression results showed

a clear linear relationship between the simulated and derived parameters in Table 15,

which was further confirmed by the fitted value plots in Figure 7. Based on the

regression results, the derivation equations of the two ratios can be further calibrated into

the form in Equation 22 and Equation 23:

$$t_p = \begin{cases} g_q - \dfrac{\ln[(1-\dfrac{v_{o,min}}{sf})(\dfrac{v_{o,max}-v_uf}{v_{o,min}-v_uf})]}{\ln(1-F)} & sf > v_{o,min} \\ 0.0 & sf < v_{o,min} \end{cases} \tag{8}$$

$$R^S{}_{pt} = 0.180 + 0.399 \cdot R^D{}_{pt} = 0.180 + 0.399 \cdot \frac{t_p}{C} \tag{22}$$

$$n_{a,p} = sf(g_q - t_b) + v_u f(t_e - g_q) + \frac{1-(1-F)^{g^q} + (1-\dfrac{1}{sf})v_{o,min} - v_{o,max}}{\ln(1-F)} \tag{15}$$

$$R^S{}_{pf} = 0.745 + 0.685 \cdot R^D{}_{pf} = 0.745 + 0.685 \cdot \frac{n_{a,p}}{v_o t_p} \tag{23}$$

The reason behind this process of calibration is that a valid connection between

the platoon variables from mathematical derivation and those from the simulation results

need to be established. Equations 22 and 23 can now be used to generate the platoon

variables directly from a real-world scenario of four-lane TWSC intersection, without

having to deal with the complex combinations of various factors.

Delay Adjustment Factors

In order to examine how the delay of MSLT movements at TWSC intersections

was affected by platoon arrivals in opposing through traffic, the concept of delay

adjustment factor was introduced in Chapter IV. From the simulation results, a dataset

for analyzing MSLT F_{da} was prepared. The dataset includes the simulated platoon time ratio, the simulated platoon flow ratio, the MSLT F_{da} and also the characteristics for each simulation scenario. Results on each row were collected and calculated from 1-hour simulations in VISSIM. The first 5 rows prepared for two-lane intersections with a LTL were shown in Table 16 as an illustration of the dataset.

Table 16 Dataset of MSLT F_{da} for Two-Lane TWSC Intersection with LTL

Speed (mph)	Distance (ft)	Red Time Portion	Signal Cycle (sec)	R^S_{pt}	R^S_{pf}	F_{da}
30	600	0.33	60	0.16	3.48	0.95
30	600	0.50	60	0.18	3.63	1.38
30	600	0.67	60	0.19	3.80	1.63
30	600	0.33	90	0.18	3.51	1.63
30	600	0.50	90	0.21	3.61	1.68

The dataset was prepared for all four scenarios: two-lane with a LTL, two-lane without a LTL, two-lane with a LTL, and four-lane without a LTL. Linear regression was employed to establish the relationship between the two platoon variables (R^S_{pt} and R^S_{pf}) and the delay adjustment factors (F_{da}). F_{da} was set as the dependent variable and the two platoon ratios were used as the independent variables. The regression results are summarized in Table 17 for each of the four scenarios.

In the regression results, the relatively higher R-squared values in four-lane major-street intersections (both with and without a LTL) indicate a relationship between the two platoon ratios and the delay adjustment factors, meaning that the characteristics of platoons are significant contributing factors to the delay changes for four-lane intersections.

Table 17 Regression Results for Platoon Variables and MSLT Delay Adjustment Factors

		Two-Lane				Four-Lane			
	Dependent Variable: F_{da}					Dependent Variable: F_{da}			
	---					---			
	Coefficients:					Coefficients:			
	Estimate	Std. Error	t value	Pr(>|t|)		Estimate	Std. Error	t value	Pr(>|t|)
Without LTL	(Intercept) 0.684	0.094	7.284	6.69e-13 ***		(Intercept) 1.900	0.083	22.92	<2e-16 ***
	R^S_{pt} 0.569	0.143	3.983	7.32e-05 ***		R^S_{pt} -2.366	0.119	-19.89	<2e-16 ***
	R^S_{pf} 0.063	0.019	3.343	0.00086 ***		R^S_{pf} -0.234	0.019	-12.42	<2e-16 ***
	---					---			
	Residual standard error:					Residual standard error:			
	0.1633 on 969 degrees of freedom					0.2054 on 969 degrees of freedom			
	Multiple R-squared: 0.01652					Multiple R-squared: 0.3141			
	Adjusted R-squared: 0.01449					Adjusted R-squared: 0.3126			
	F-statistic: 8.137 on 2 and 969 DF					F-statistic: 221.8 on 2 and 969 DF			
	p-value: 0.0003131					p-value: < 2.2e-16			
	Dependent Variable: F_{da}					Dependent Variable: F_{da}			
	---					---			
	Coefficients:					Coefficients:			
	Estimate	Std. Error	t value	Pr(>|t|)		Estimate	Std. Error	t value	Pr(>|t|)
With LTL	(Intercept) 0.342	0.123	2.781	0.00553 **		(Intercept) 1.860	0.082	22.77	<2e-16 ***
	R^S_{pt} 1.319	0.187	7.069	2.98e-12 ***		R^S_{pt} -2.383	0.117	-20.36	<2e-16 ***
	R^S_{pf} 0.125	0.025	5.090	4.29e-07 ***		R^S_{pf} -0.220	0.019	-11.81	<2e-16 ***
	---					---			
	Residual standard error:					Residual standard error:			
	0.2115 on 969 degrees of freedom					0.2036 on 969 degrees of freedom			
	Multiple R-squared: 0.0585					Multiple R-squared: 0.335			
	Adjusted R-squared: 0.05655					Adjusted R-squared: 0.3336			
	F-statistic: 30.1 on 2 and 969 DF					F-statistic: 244.1 on 2 and 969 DF			
	p-value: 2.074e-13					p-value: < 2.2e-16			

This relationship of four-lane intersections could be observed in Figure 8. Figure 8 presents the plots of simulated F_{da}s and that fitted using the linear regression model. Perfect fitted plot will have the points spreading around the 45 degree line. Based on the relationship existing at four-lane intersections, the delay adjustment factors for MSLT movement could be estimated with the platoon time ratio and the platoon flow ratio. The details of the examination on the relationships listed in Appendix D.
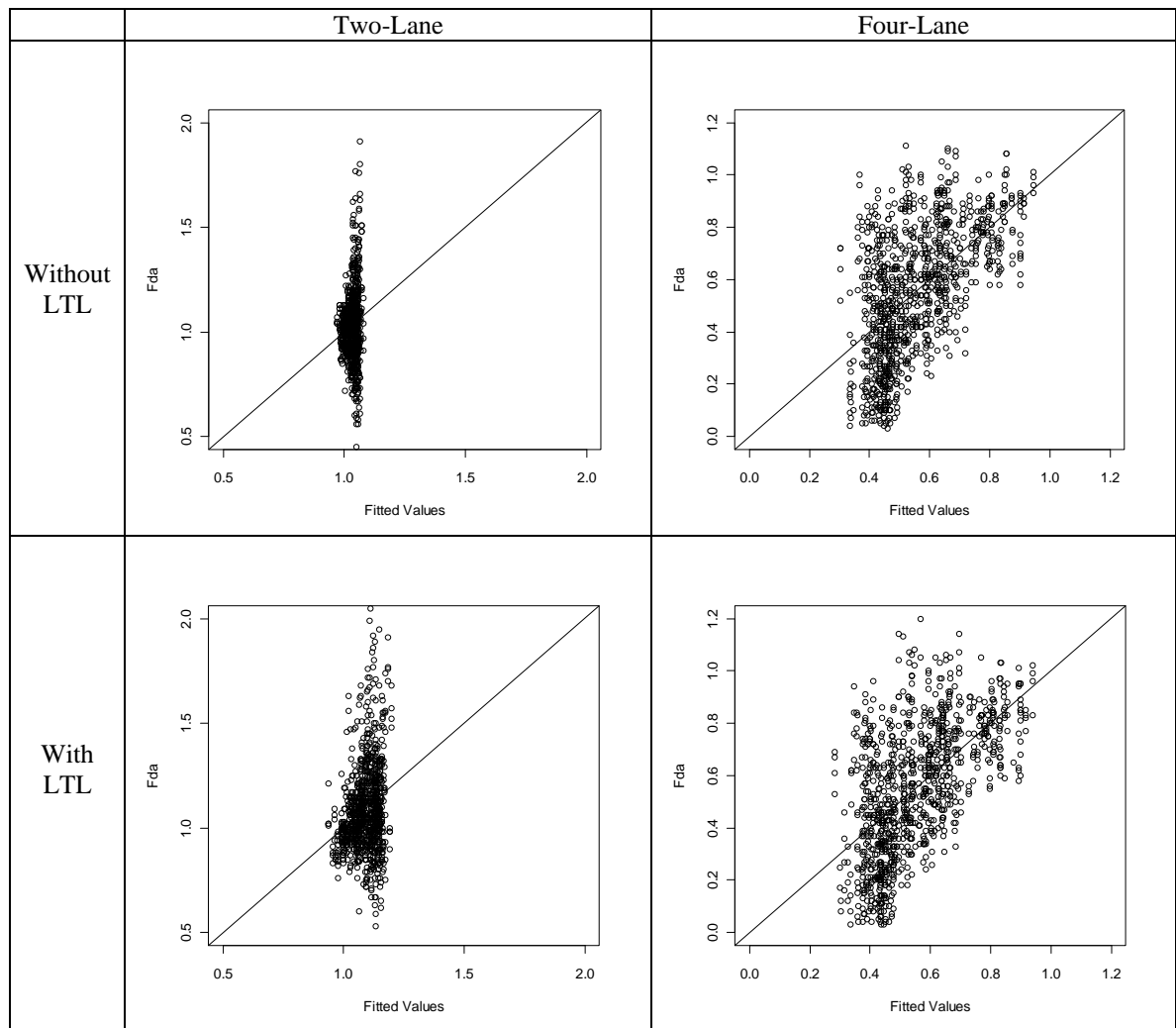
Figure 8 MSLT Delay Adjustment Factors vs. Values Fitted by Regression

The fit for two-lane major-street intersections is not adequate to establish the correlation between the platoon ratios and the delay adjustment factors. Therefore, no clear relationship between the platoons and the delay changes was found in two-lane major-street intersections. Possible reasons include that the platoons form automatically on two-lane roads. Vehicles on the two-lane roads cannot change lane and pass the slow vehicle in front, therefore platoon are formed automatically after a while even if no

traffic signals is present. Because platoons always exist on two-lane roads, no evident impacts on delay by the upstream platoon arrivals generated by traffic signal were observed. Another fact that may lead to this result is that the gap distributions of traffic on two-lane and four-lane roads are actually quite different.

For four-lane major-street intersections, the relationships between the platoon variables and the delay adjustment factors have been established, and linear regression equations can be used to describe the relationship:

$$F_{da} = 1.900 - 2.366 R^S{}_{pt} - 0.234 R^S{}_{pf} \text{ , without LTL} \qquad (24)$$

$$F_{da} = 1.860 - 2.383 R^S{}_{pt} - 0.220 R^S{}_{pf} \text{ , with LTL} \qquad (25)$$

Equations 24 and 25 give almost the same results while the two independent variables values stay in the normal range, meaning that no significant difference exists between the equations. Since the presence of left-turn lane does not affect the platoon impacts on MSLT delay, either of the two equations can be used as the formula for further analysis.

Based on Equation 24, a 3-D plot was plotted in Figure 9 and a table for looking-up delay adjustment factors by platoon variables was prepared in Table 18. From both Figure 9 and Table 18, positive effects of platoon arrivals in opposing through traffic on MSLT delay can be seen. Except for some unreasonable combinations of platoon variables (the two platoon variables cannot reach the extreme values at the same time), the F_{da}s are smaller than 1, meaning that the MSLT delay is reduced by the platoon

arrivals from upstream opposing traffic. Moreover, as the duration intensities of the platoons increase, the positive effect is also stronger. Table 18 can also be used for TWSC intersections' left-turn treatment design regarding the upstream traffic signal's impacts.
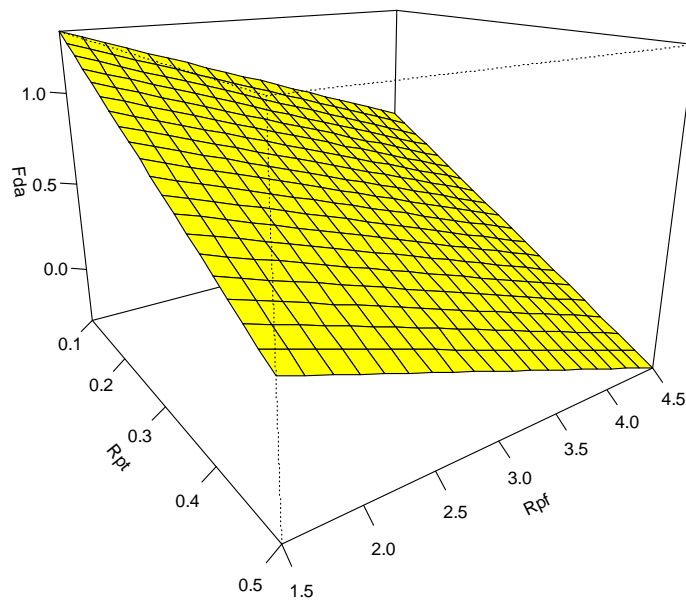
Figure 9 3-D Plot of Delay Adjustment Factors for Four-Lane TWSC Intersections

Table 18 Delay Adjustment Factors of MSLT Movement for Four-Lane TWSC Intersections

R_{pf}	$R_{p,t}$								
	0.1	0.15	0.2	0.25	0.3	0.35	0.4	0.45	0.5
1.5	1.31	1.19	1.08	0.96	0.84	0.72	0.6	0.48	0.37
2	1.2	1.08	0.96	0.84	0.72	0.6	0.49	0.37	0.25
2.5	1.08	0.96	0.84	0.72	0.6	0.49	0.37	0.25	0.13
3	0.96	0.84	0.72	0.61	0.49	0.37	0.25	0.13	0.01
3.5	0.84	0.73	0.61	0.49	0.37	0.25	0.13	0.02	NA
4	0.73	0.61	0.49	0.37	0.25	0.14	0.02	NA	NA
4.5	0.61	0.49	0.37	0.26	0.14	0.02	NA	NA	NA
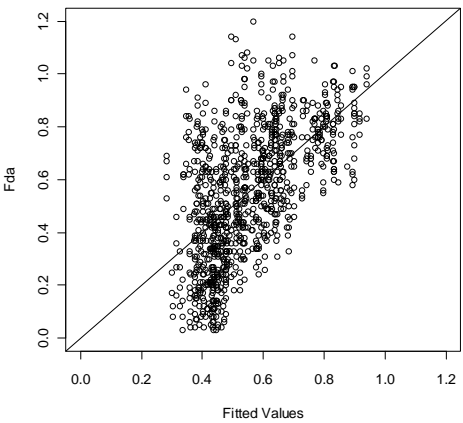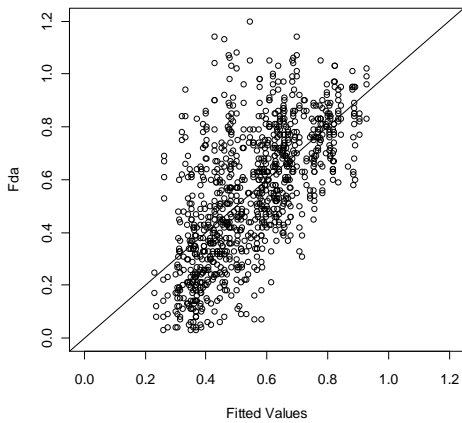
*Note: 1. Delay Adjustment Factors smaller than 0 are replaced with NAs

2. R_{pt} ranges from 0.13 to 0.49, R_{pf} range from 1.60 to 4.42

3. ▇ $0.66 <= F_{da} < 1$ ▇ $0.33 <= F_{da} < 0.66$ ▇ $0 < F_{da} < 0.33$

Procedure of using the developed methodology to determine MSLT delay change due to platoon at a four-lane TWSC intersection is as follows: for any platoon scenario, firstly, apply Equation 22 and 23 to calculate the two platoon variables, which describe the duration and intensity of the platoon arrivals; secondly, use Table 18 or Equation 24 and 25 to get the delay adjustment factor, which is a quantitative description of how the platoons affect the MSLT delay.

Four two-lane major-street intersections, no significant effects of platooning traffic on left-turn delay were found in the analysis. It is probably due to the ability of two-lane major-street to form multiple platoons automatically. Vehicles on the two-lane roads cannot change lane and pass the slow vehicle in front, therefore platoon are formed automatically after a while even if no traffic signals is present. Also the low volume at the unsignalized intersection might be also part of the reason.
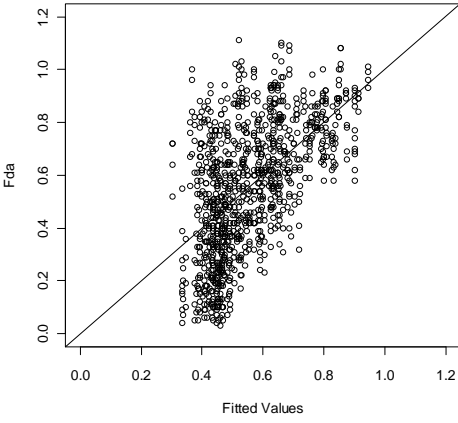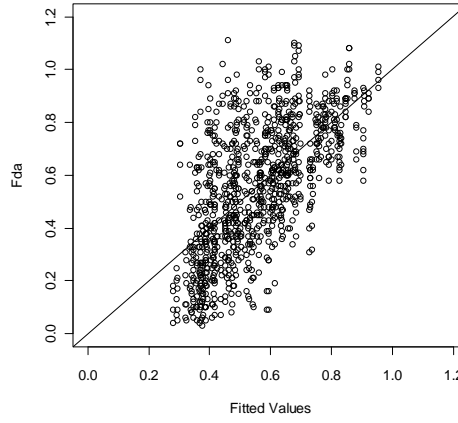
Further improvement work was conducted for four-lane TWSC intersections. For the regressions that have been applied, the independent variables R^S_{pt} and R^S_{pt} were transformed with Box-Cox transformation. The regression results and fitted value plots were summarized in Table 19 for both old model and new model.

Table 19 Comparison of Models for Four-Lane TWSC Intersections with LTL

Four-Lane with LTL	
Coefficients: Estimate Std. Error t value Pr(>|t|) (Intercept) 1.860 0.082 22.77 <2e-16 *** R^S_{pt} -2.383 0.117 -20.36 <2e-16 *** R^S_{pf} -0.220 0.019 -11.81 <2e-16 *** --- Residual standard error: 0.2036 on 969 degrees of freedom Multiple R-squared: 0.335 Adjusted R-squared: 0.3336 F-statistic: 244.1 on 2 and 969 DF, p-value: < 2.2e-16	Coefficients: Estimate Std. Error t value Pr(>|t|) (Intercept) 0.908 0.01693 53.66 <2e-16 *** RSpt 1.3 -3.255 0.13354 -24.37 <2e-16 *** RSpf -2.6 3.535 0.21207 16.67 <2e-16 *** --- Residual standard error: 0.193 on 969 degrees of freedom Multiple R-squared: 0.4025 Adjusted R-squared: 0.4013 F-statistic: 326.4 on 2 and 969 DF, p-value: < 2.2e-16

For four-lane intersections with LTL shown in Table 19, the R squared values was increased from 0.33 to 0.40, and the fitted value plot also showed a better fit to the 45 degree line. These indicate that this new model is a better fit than the old model. The similar results were observed for four-lane intersections without LTL summarized in Table 20.

Table 20 Comparison of Models for Four-Lane TWSC Intersections without LTL

Four-Lane without LTL	
Coefficients: Estimate Std. Error t value Pr(>|t|) (Intercept) 1.900 0.083 22.92 <2e-16 *** R^S_{pt} -2.366 0.119 -19.89 <2e-16 *** R^S_{pf} -0.234 0.019 -12.42 <2e-16 *** --- Residual standard error: 0.2054 on 969 degrees of freedom Multiple R-squared: 0.3141 Adjusted R-squared: 0.3126 F-statistic: 221.8 on 2 and 969 DF, p-value: < 2.2e-16	Coefficients: Estimate Std. Error t value Pr(>|t|) (Intercept) 0.946 0.019 48.54 <2e-16 *** $R^{S\ 1.1}_{pt}$ -2.965 0.125 -23.63 <2e-16 *** $R^{S\ -2.2}_{pf}$ 3.013 0.180 16.77 <2e-16 *** --- Residual standard error: 0.195 on 969 degrees of freedom Multiple R-squared: 0.3816 Adjusted R-squared: 0.3803 F-statistic: 299 on 2 and 969 DF, p-value: < 2.2e-16

With the new regression model, the delay adjustment factors for MSLT movement could be estimated with the platoon time ratio and the platoon flow ratio as shown in Equation 26 and 27 for four-lane TWSC intersection with and without left-turn lane. Also the delay adjustment factors were re-calculated and summarized in Table 21 and Table 22. The results calculated from the new model were considered to perform better than that from the old model, and should be used in the analysis.

$$F_{da} = 0.946 - 2.965 R^S_{pt}{}^{1.1} + 3.013 \frac{1}{R^S_{pf}{}^{2.2}} \qquad \text{,without LTL} \qquad (26)$$

$$F_{da} = 0.908 - 3.255 R^S_{pt}{}^{1.3} - 3.535 \frac{1}{R^S_{pf}{}^{2.6}} \qquad \text{, with LTL} \qquad (27)$$

Table 21 Delay Adjustment Factors of MSLT Movement for Four-Lane TWSC Intersections with LTL

R_{pf}	$R_{p,t}$								
	0.1	0.15	0.2	0.25	0.3	0.35	0.4	0.45	0.5
1.5	1.95	1.81	1.68	1.54	1.39	1.25	1.1	0.95	0.8
2	1.37	1.23	1.1	0.96	0.81	0.67	0.52	0.37	0.22
2.5	1.11	0.98	0.84	0.7	0.56	0.41	0.27	0.12	NA
3	0.98	0.85	0.71	0.57	0.43	0.28	0.13	NA	NA
3.5	0.9	0.77	0.63	0.49	0.35	0.2	0.06	NA	NA
4	0.85	0.72	0.58	0.44	0.3	0.15	0.01	NA	NA
4.5	0.82	0.69	0.55	0.41	0.27	0.12	NA	NA	NA

*Note: 1. Delay Adjustment Factors smaller than 0 are replaced with NAs
2. R_{pt} ranges from 0.13 to 0.49, R_{pf} range from 1.60 to 4.42
3. ▢ $0.66 <= F_{da} < 1$ ▢ $0.33 <= F_{da} < 0.66$ ▢ $0 < F_{da} < 0.33$

Table 22 Delay Adjustment Factors of MSLT Movement for Four-Lane TWSC Intersection without LTL

R_{pf}	$R_{p,t}$								
	0.1	*0.15*	*0.2*	*0.25*	*0.3*	*0.35*	*0.4*	*0.45*	*0.5*
1.5	1.98	1.86	1.74	1.6	1.46	1.31	1.15	0.99	0.82
2	1.33	1.21	1.09	0.95	0.81	0.66	0.5	0.34	0.17
2.5	1.07	0.96	0.83	0.7	0.55	0.4	0.25	0.08	NA
3	0.95	0.84	0.71	0.57	0.43	0.28	0.12	NA	NA
3.5	0.88	0.77	0.64	0.51	0.36	0.21	0.06	NA	NA
4	0.84	0.73	0.6	0.47	0.32	0.17	0.02	NA	NA
4.5	0.82	0.7	0.58	0.44	0.3	0.15	NA	NA	NA

*Note: 1. Delay Adjustment Factors smaller than 0 are replaced with NAs
2. R_{pt} ranges from 0.13 to 0.49, R_{pf} range from 1.60 to 4.42
3. ⬜ $0.66 <= F_{da} < 1$ 🟦 $0.33 <= F_{da} < 0.66$ 🟦 $0 < F_{da} < 0.33$

Based on the new results, an updated procedure of using the developed methodology to determine MSLT delay change due to platoon at a four-lane TWSC intersection is as follows:

- First, apply the platoon variable equations in Equation 22 and 23 to calculate the two platoon variables, which describe the duration and intensity of the platoon arrivals;

- Second, use equations in Equation 26 and 27 or values in Table 21 and 22 to get the delay adjustment factor, which is a quantitative description of how the platoons affect the MSLT delay.

CHAPTER VI

CONCLUSIONS

This research aims to evaluate the impacts of platoons generated from the upstream intersection on major-street left-turn delay at downstream unsignalized intersections. The study defined two ratios to describe different platoon scenarios and established a relationship between the two platoon ratios on the delay reduction for major-street left-turn delay based on VISSIM simulation results. Those two ratios are R_{pt} and R_{pf}, describing the platoon intensity from the aspect of time and flow volume respectively. A further critical gap calibration based on field data was also performed in this research. Raff's model and logistic regression model were employed to calibrate the critical gap for each intersection, and the better one of the two above was selected with the help of VISSIM simulation. More detailed critical gaps for major-street left-turn at two-lane stop-control intersections were recommended based on the analysis of related factors. The following are the main findings from this research:

- For two-lane TWSC unsgianlized intersections, there were no evident impacts on major-street left-turn delay by platoons in opposing through traffic generated from the upstream signalized intersection found in this research.

- For four-lane TWSC unsignalized intersections, the platoons have shown a positive effect on left-turn delay, which reduces the left-turn delay. Furthermore, as the intensity of the platoon goes up, the positive effect gets stronger and the

delay saving percentage increases. The platoon impact can be quantified using the methodology proposed in this research.

- For treatment at unsignalized intersection, an adjustment on the volume warrants based on the platoon impacts should be adopted. Basically, the critical volumes can be increased at unsignalized intersection with platooning arrivals.

- The posted speed has a significant impact on critical gaps; specifically, the critical gap increases with the posted speed limits. Four-lane intersections have larger critical gap than two-lane intersections. One more thing noticed from this research was that for critical gap calibration, the Raff's model is preferred unless other sophisticated models could give significantly better results.

CHAPTER VII

LIMITATIONS AND FUTURE WORK

The first limitation of this research is that the analysis was based on the simulation data. There's still difference between the simulation work and the real-world situation, although VISSIM used in this research is one of the leading tools for traffic simulation. If the data can be collected from the real-world platoon scenarios, the reliability of the whole work will be increased.

Also the statistics analysis in this research is using simple tools like T test and linear regression models. The statistics analysis can be done using more sophisticated techniques for improvement in the future.

REFERENCES

1. *Highway Capacity Manual, 3rd ed.* TRB, National Research Council, Washington, D.C., 2000.

2. Bonneson, J. A., and J. W. Fitts. Effect of Upstream Signal on Nonpriority Movement Capacity and Delay. In *Transportation Research Record 1572*, TRB, National Research Council, Washington, D.C., 1996, pp. 174-182.

3. Robinson, B. W., Z. Tian, W. Kittelson, M. Vandehey, M. Kyte, W. Brilon, et al. Extensions of Theoretical Capacity Models to Account for Special Conditions. *Transportation Research Part A,* No. 33, 1999, pp. 217-236.

4. Dell'Olmo, P., and P. B. Mirchandani. REALBAND: An Approach for Real-Time Coordination of Traffic Flows on Networks. *Transportation Research Record 1494*, TRB, National Research Council, Washington, D.C., 1995, pp. 106-116.

5. Gaur, A., and P. Mirchandani. Method for Real-Time Recognition of Vehicle Platoons. *Transportation Research Record 1748*, TRB, National Research Council, Washington, D.C., 2001, pp. 8-16.

6. Robertson, D. I. TRANSYT: A Traffic Network Study Tool. British Road Research Laboratory, Wokingham Berkshire, U.K., 1969.

7. Rouphail, N. M. Analysis of TRANSYT Platoon-Dispersion Algorithm. *Transportation Research Record 905* , TRB, National Research Council, Washington, D.C., 1983, pp. 72-80.

8. Harmelink, M. D. Volume Warrants for Left-Turn Storage Lanes at Unsignalized Grade Intersections. In *Highway Research Record 211*, HRB, National Research Council, Washington, D.C., 1967, pp. 1-18.

9. Fitzpatrick, K., and T. Wolff. Left-Turn Lane Installation Guidelines. *2nd Urban Street Symposium.* Anaheim, California, 2003.

10. Ranade, S., A. W. Sadek, and J. N. Ivan. Decision Support System for Predicting Benefits of Left-Turn Lanes at Unsignalized Intersections. *Transportation Research Record 2023*, TRB, National Research Council, Washington, D.C.,2007, pp. 28-36.

11. Gluck, J., H. S. Levinson, and V. Stover. *Impacts of Access Management Techniques.* NCHRP Report 420, Transportation Research Board, Washington, D.C., 1999.

12. Maze, T. H., J. L. Henderson, and S. Sankar. *Impacts on safety of left-turn treatment at highspeed signalized intersections.* Project HR-347, Iowa Highway Research Board. Ames, Iowa, 1994.

13. Agent, K. Warrants For Left-Turn Lanes. *Transportation Quarterly*, Vol. 37, No.1, 1983, pp. 99–114.

14. McCoy, P. T., and M. S. Malone. Safety Effects Of Left-Turn Lanes On Urban Four-Lane Roadways. *Transportation Research Record 1239*, TRB, National Research Council, Washington, D.C., 1989, pp. 17–22.

15. Harwood, D. W., K. M. Bauer, I. B. Potts, D. J. Torbic, K. R. Richard, E. R. Kohlman Rabbani, E. Hauer, and L. Elefteriadou. *Safety Effectiveness of Intersection Left- and Right-Turn Lanes.* Report FHWARD-02-089. FHWA, U.S. Department of Transportation, 2002.

16. Brilon, W., K. Ralph, and J. T. Rod. Useful Estimation Procedures for Critical Gaps. *Transportation Research Part A*, Vol. 33, No. 3-4, 1999, pp. 161-186.

17. Lee, J., F.L.Mannering. Impact of Roadside Features on The Frequency and Severity of Run-Off-Roadside Accidents: An Empirical Analysis. *Accident Analysis and Prevention,* Vol. 34, No. 2, 2002, pp. 149–161.

18. Chang, L. Y., and F. L. Mannering. Analysis of Injury Severity and Vehicle Occupancy in Truck and Non-Truck Involved Accidents. *Accident Analysis and Prevention*, Vol. 31, No. 5, 1999, pp. 579-592.

19. Polus, A., Y. Shiftan, and S. Shmueli-Lazar. Evaluation of the Waiting-Time effect on Critical Gaps at Roundabouts by a Logit Model. *European Journal of Transport and Infrastructure Research*, Vol. 5, No. 1, 2005, pp. 1-12.

20. Kittelson, W. K., and M. A Vandehey. Delay Effects on Driver Gap Acceptance Characteristics at Two-Way Stop-Controlled Intersections. *Transportation Research Record 1320*, TRB, National Research Council, Washington, D.C.,1991, pp. 154-159.

21. Dissanayake, S., J. J. Lu, and P. Yi. Driver Age Differences in Day and Night Gap Acceptance Capabilities. *IATSS Research*, Vol. 26, No. 1, 2002, pp. 71-79.

22. Yan, X, E. Radwan, and D. Guo. Effects of Major-Road Vehicle Speed and Driver Age and Gender on Left-Turn Gap Acceptance. *Crash Analysis and Prevention,* Vol. 39, No. 4, 2007, pp. 843-852

23. *VISSIM 5.10 User Manual.* Planung Transport Verkehr, Karlsruhe, Germany, 2008.

24. S.J. Sheather. *A Modern Approach to Regression with R*. Springer Science + Business Media LLC, Philadelphia, PA, 2009

APPENDIX A

The detailed derivation process for Equation 15 is documented below. The variable $n_{a,p}$ is the number of vehicles within one cycle as shown in Figure A, which is the area circled by the red line in Figure A.

$$n_{a,p} = sf(g_q - t_b) + v_u f(t_e - g_q) + \frac{1-(1-F)^{g^q} + (1-\frac{1}{sf})v_{o,min} - v_{o,max}}{\ln(1-F)} \qquad (15)$$
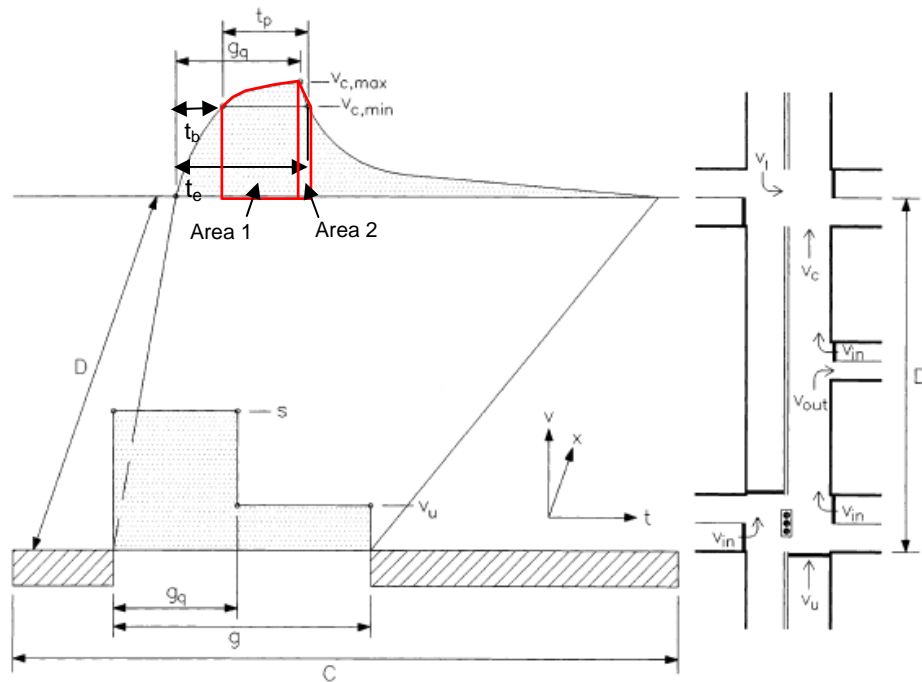

Figure A: Platoon Dispersion Model Characteristics (Bonnesson, 1996)

For area 1:

$$n_1 = \int_{t_b}^{g_q} sf(1-(1-F)^t)dt$$

$$n_1 = \int_{t_b}^{g_q} sf dt - \int_{t_b}^{g_q} (1-F)^t \, dt$$

$$n_1 = sf(g_q - t_b) - \int_{t_b}^{g_q} e^{t \log(1-F)} \, dt$$

$$n_1 = sf(g_q - t_b) - \frac{1}{\log(1-F)}((1-F)^{g_q} - (1-F)^{t_b})$$

For area 2:

$$n_2 = \int_{g_q}^{t_e} v_u f + (v_{o,\max} - v_u f)(1-F)^{t-g_q} \, dt$$

$$n_2 = v_u f(t_e - g_q) + (v_{o,\max} - v_u f) \int_{g_q}^{t_e} (1-F)^{t-g_q} \, dt$$

$$n_2 = v_u f(t_e - g_q) + (v_{o,\max} - v_u f) \int_{g_q}^{t_e} e^{(t-g_q)\log(1-F)} \, d(t-g_q)$$

$$n_2 = v_u f(t_e - g_q) + \frac{(v_{o,\max} - v_u f)}{\log(1-F)}(1-F)^{t-g_q} \Big|_{g_q}^{t_e}$$

$$n_2 = v_u f(t_e - g_q) + \frac{(v_{o,\max} - v_u f)}{\log(1-F)}((1-F)^{t_e - g_q} - 1)$$

Solve for t_b:

$$sf(1 - (1-F)^t) = v_{o,\min}$$

$$(1-F)^t = 1 - \frac{v_{o,\min}}{sf}$$

$$t \log(1-F) = \log(1 - \frac{v_{o,\min}}{sf})$$

$$t = \frac{\log(1 - \frac{v_{o,\min}}{sf})}{\log(1-F)}$$

$$t_b = \frac{\log(1 - \frac{v_{o,\min}}{sf})}{\log(1-F)}$$

Solve for t_e:

$$v_u f + (v_{o,\max} - v_u f)(1-F)^{(t-g_q)} = v_{o,\min}$$

$$(1-F)^{(t-g_q)} = \frac{v_{o,\min} - v_u f}{v_{o,\max} - v_u f}$$

$$t = \log \frac{v_{o,\min} - v_u f}{v_{o,\max} - v_u f} / \log(1-F) + q_g$$

$$t_e = \log \frac{v_{o,\min} - v_u f}{v_{o,\max} - v_u f} / \log(1-F) + q_g$$

The total area:

$$n_{a,p} = n_1 + n_2$$

$$n_{a,p} = sf(g_q - t_b) - \frac{1}{\log(1-F)}((1-F)^{g_q} - (1-F)^{t_b})$$

$$+ v_u f(t_e - g_q) + \frac{(v_{o,\max} - v_u f)}{\log(1-F)}((1-F)^{t_e - g_q} - 1)$$

$$n_{a,p} = sf(g_q - t_b) - \frac{1}{\log(1-F)}((1-F)^{g_q} - (1-F)^{\frac{\log(1-\frac{v_{o,min}}{sf})}{\log(1-F)}})$$

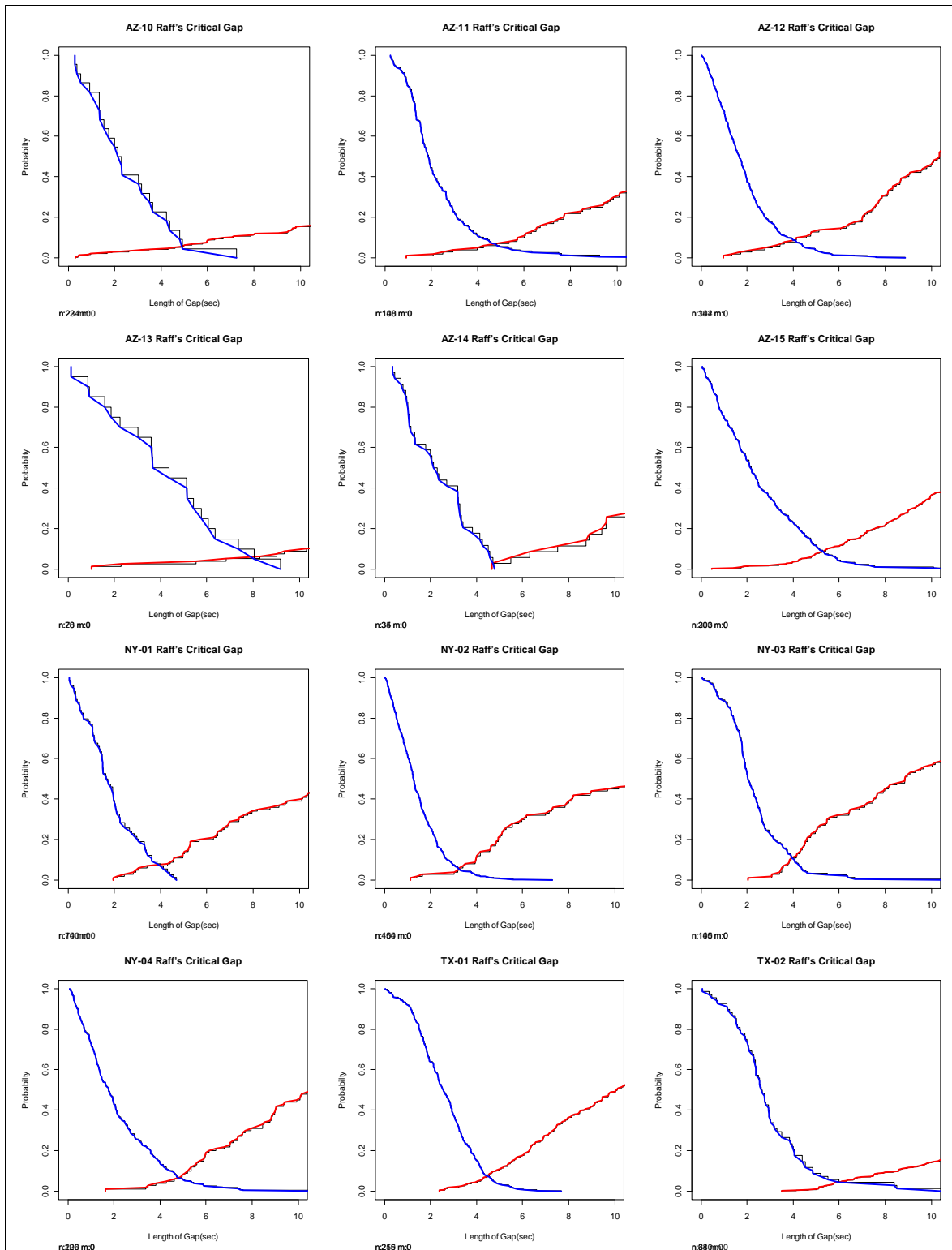$$+v_u f(t_e - g_q) + \frac{(v_{o,max} - v_u f)}{\log(1-F)}((1-F)^{\log\frac{v_{o,min} - v_u f}{v_{o,max} - v_u f}/\log(1-F)} - 1)$$

$$n_{a,p} = sf(g_q - t_b) - \frac{1}{\log(1-F)}((1-F)^{g_q} - 1 + \frac{v_{o.min}}{sf})$$

$$+v_u f(t_e - g_q) + \frac{(v_{o,max} - v_u f)}{\log(1-F)}(\frac{v_{o,min} - v_u f}{v_{o,max} - v_u f} - 1)$$

$$n_{a,p} = sf(g_q - t_b) - \frac{(1-F)^{g_q} - 1 + \frac{v_{o,min}}{sf})}{\log(1-F)} + v_u f(t_e - g_q) + \frac{v_{o,min} - v_{o,max}}{\log(1-F)}$$

$$n_{a,p} = sf(g_q - t_b) + v_u f(t_e - g_q) + \frac{1 - (1-F)^{g_q} + (1 - \frac{1}{sf})v_{o,min} - v_{o,max}}{\ln(1-F)}$$
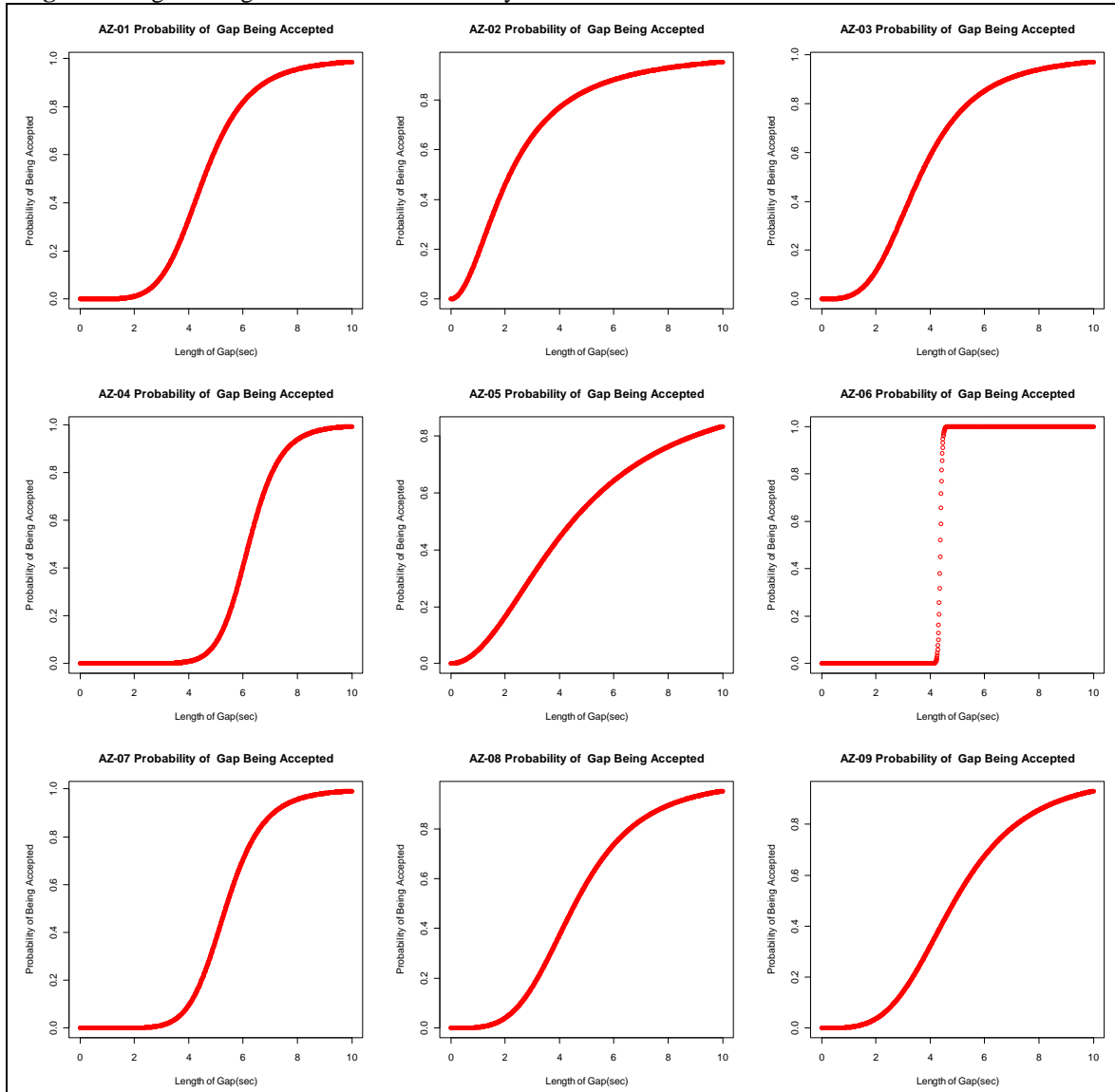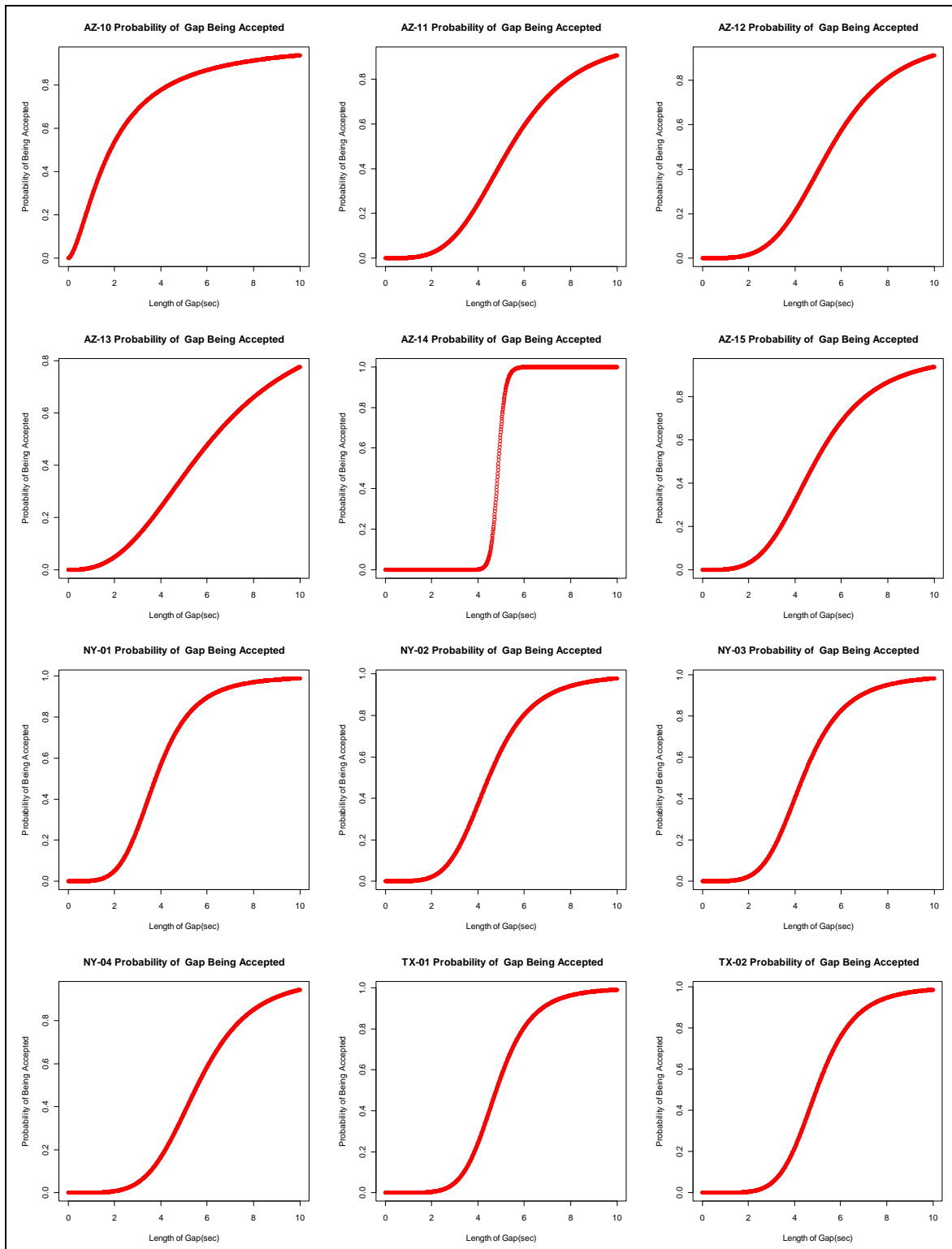
APPENDIX B

**Figure B** Raff's Critical Gap Model Plots for All 30 TWSC Intersections

TX-03 Raff's Critical Gap

TX-04 Raff's Critical Gap

TX-05 Raff's Critical Gap

TX-06 Raff's Critical Gap

TX-07 Raff's Critical Gap

TX-08 Raff's Critical Gap

TX-09 Raff's Critical Gap

TX-10 Raff's Critical Gap

TX-11 Raff's Critical Gap
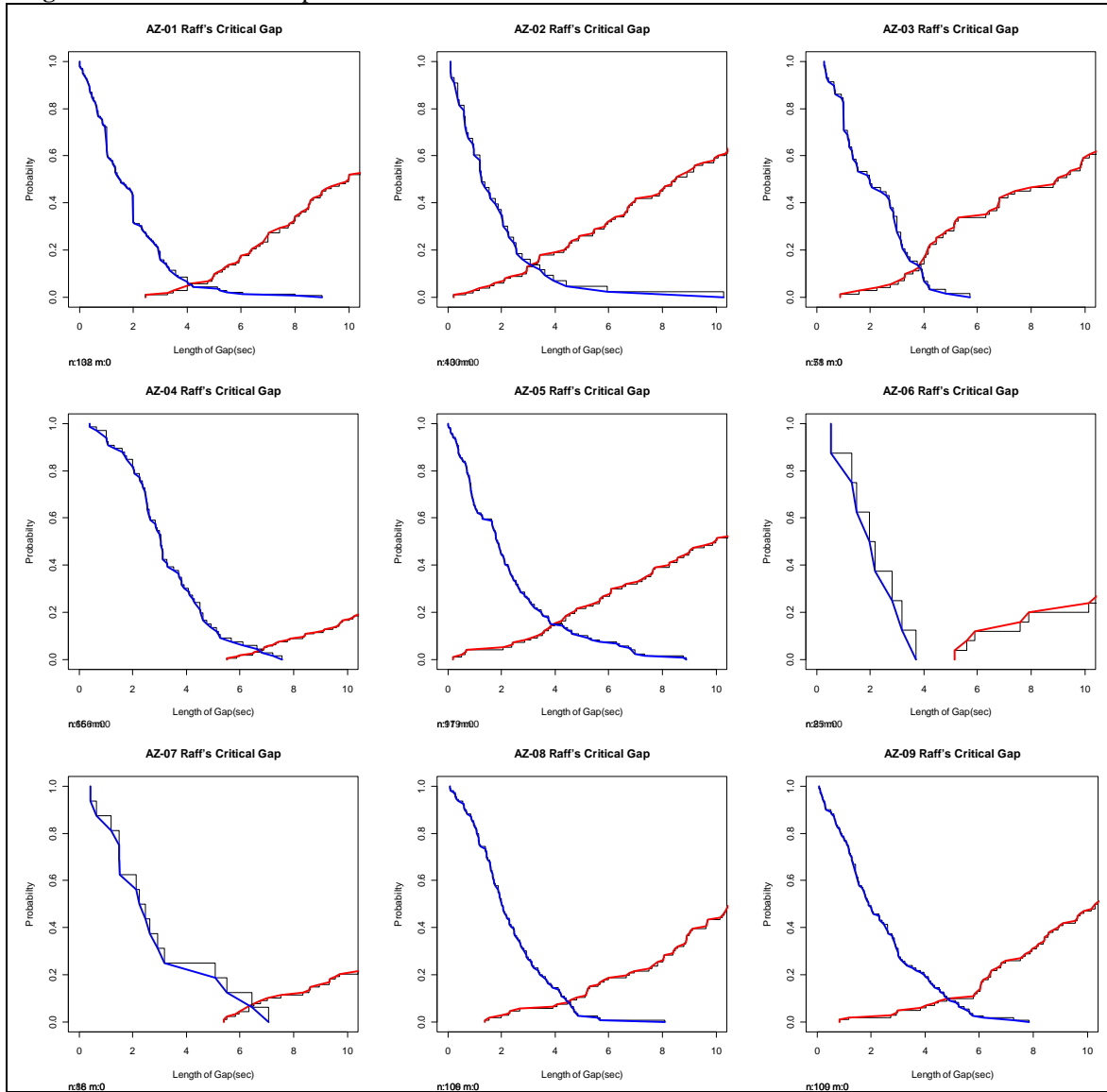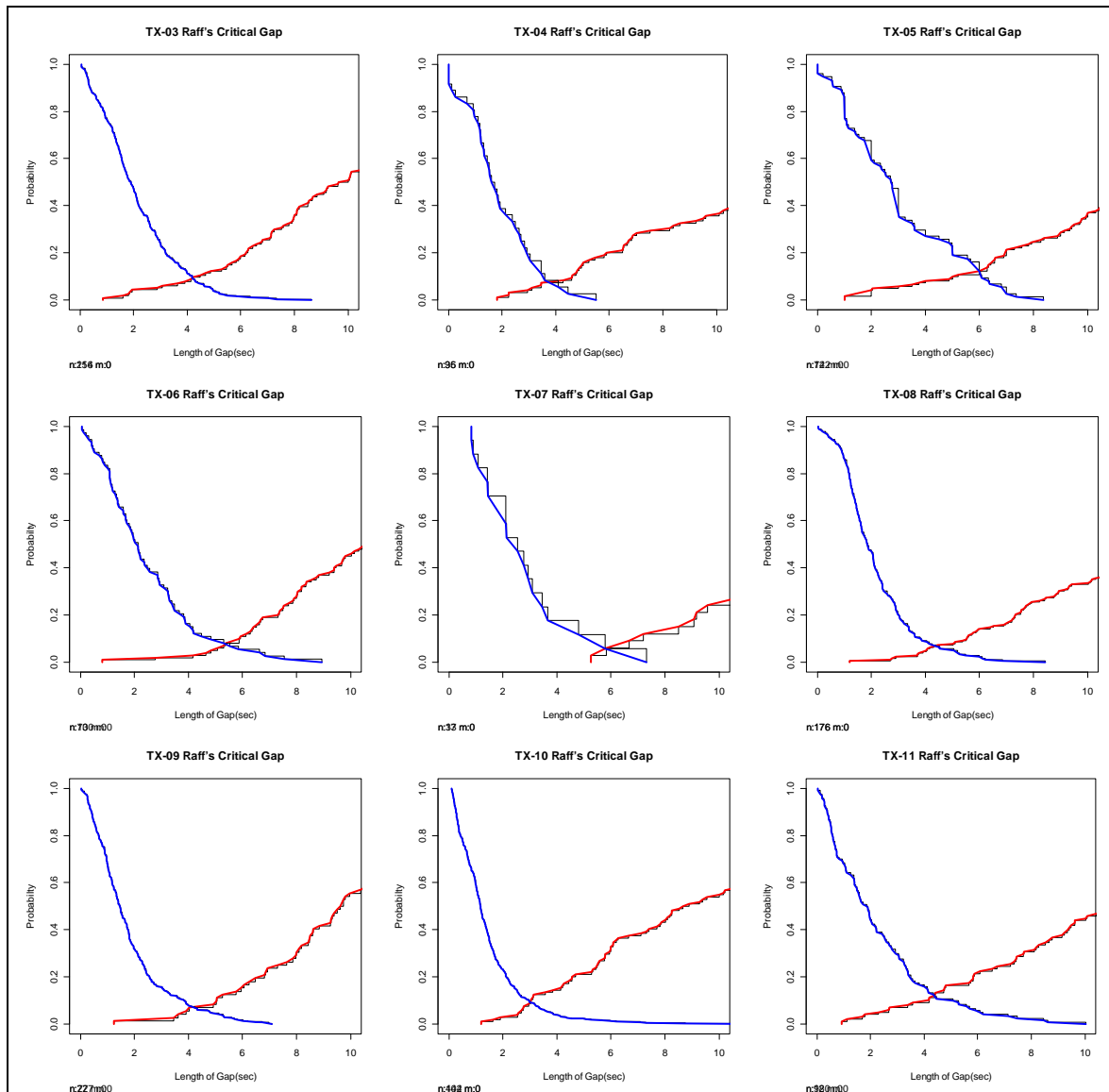
APPENDIX C

Figure C Logistic Regression Model Probability Plots for All 30 TWSC Intersections
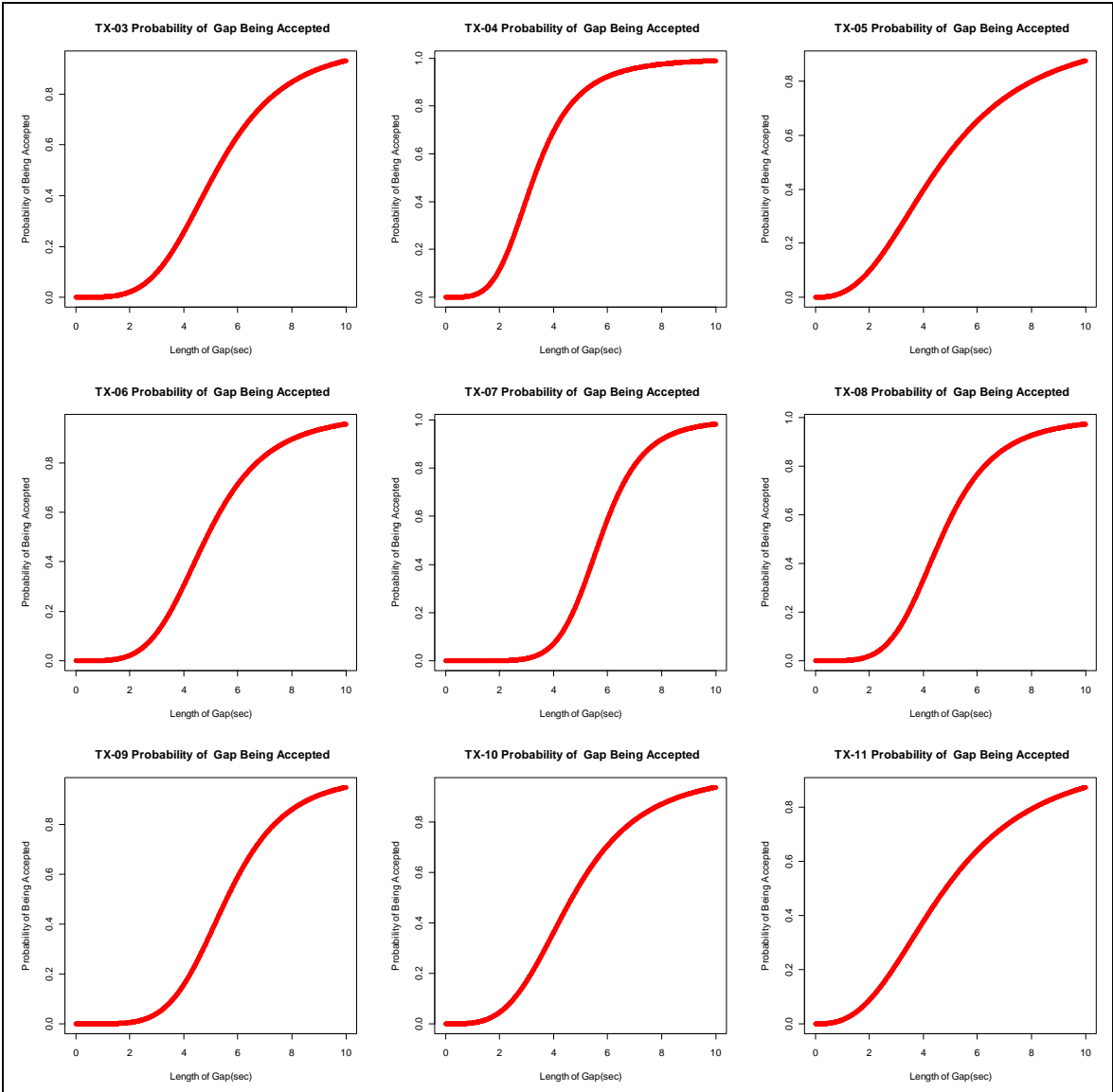
APPENDIX D

Figure D.1. Examination on Relationship bet. F_{da} and R^S_{pt} and R^S_{pf} for Four-Lane without-LTL TWSC Intersections
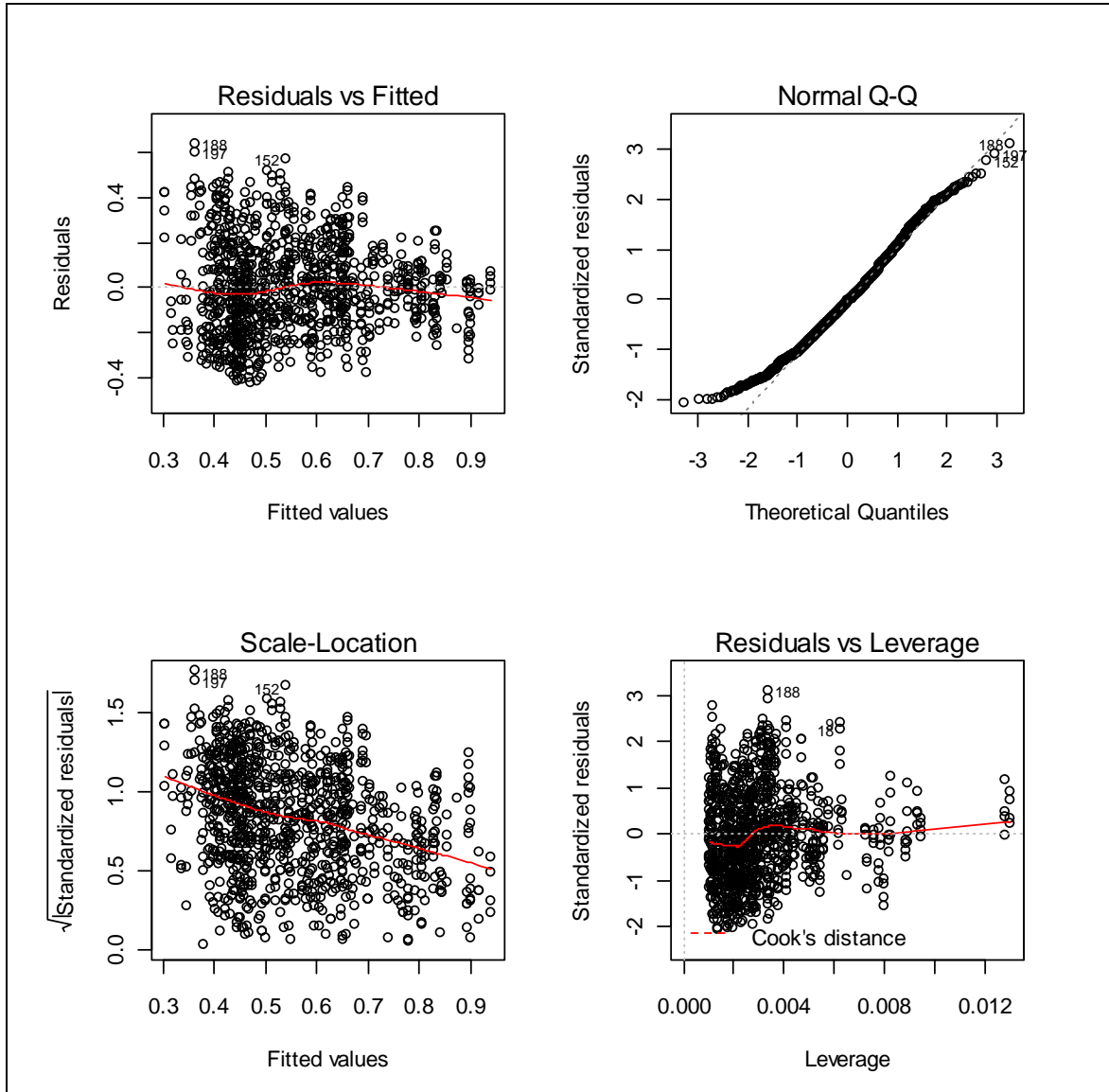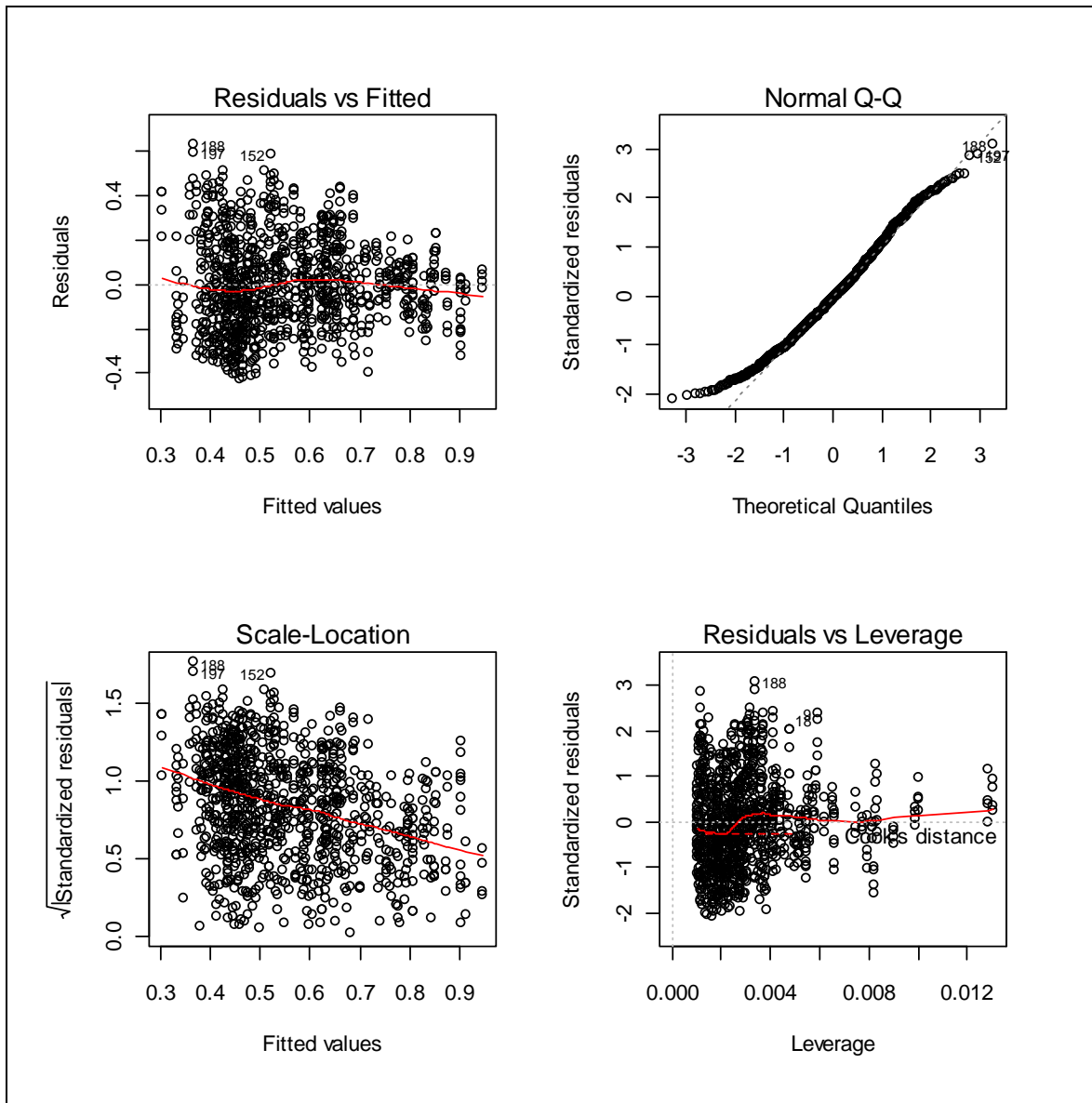
Figure D.2. Examination on Relationship between F_{da} and R^S_{pt} and R^S_{pf} for Four-Lane with-LTL TWSC

Intersections

VITA

Name: Feng Wan

Address: Department of Civil Engineering
                   c/o Dr. Yunlong Zhang
                   Texas A&M University
                   College Station, TX 77843-3136

Email Address: wanfenghuaian@hotmail.com

Education: B.S., Transportation Engineering, Tongji University, 2008
                   M.S., Civil Engineering, Texas A&M University, 2010